414) as a green fluorescent protein (GFP)-fusion [34,35]. Its expression also results in the formation of anti-pS409/410- and anti-Ub-positive inclusions. Six hours after transfection, the cells were treated with MB (Sigma–Aldrich, St. Louis, USA) dissolved in dimethyl sulfoxide (DMSO), dimebon dissolved in sterile distilled water (DW) or MB + dimebon and cultured for 3 days. As controls, cells were treated with either DMSO or DW, or both of them for 3 days.

2.3. Immunohistochemical analysis

SH-SY5Y cells were grown on coverslips and transfected as described [33]. After incubation for the indicated times, the cells were fixed with 4% paraformaldehyde and stained with anti-phosphorylated TDP-43 antibody pS409/410 or anti-Ub, followed by Alexa Fluor 488- or Alexa Fluor 568-labeled IgG (Invitrogen, Carlsbad, USA). After washing, the cells were further incubated with TO-PRO-3 (Invitrogen, Carlsbad, USA) to stain nuclear DNA. To quantify the cells with TDP-43 aggregates, the laser power (at 488 nm for detection of Alexa Fluor 488 and GFP) was adjusted, so that only aggregates were detected as described [34]. Total intensity of fluorescence detected at the threshold laser power and that of TO-PRO-3 fluorescence, the latter corresponding to the total number of cells in a given field (approximately 800 μm × 800 μm), were measured with LSM5 Pascal v 4.0 software (Carl Zeiss), and the ratio of cells with inclusions calculated.

2.4. Immunoblot analysis

Tris saline (TS)-soluble, Triton X-100 (TX)-soluble and Sarkosyl (Sar)-soluble fractions, as well as the final pellet, were prepared,

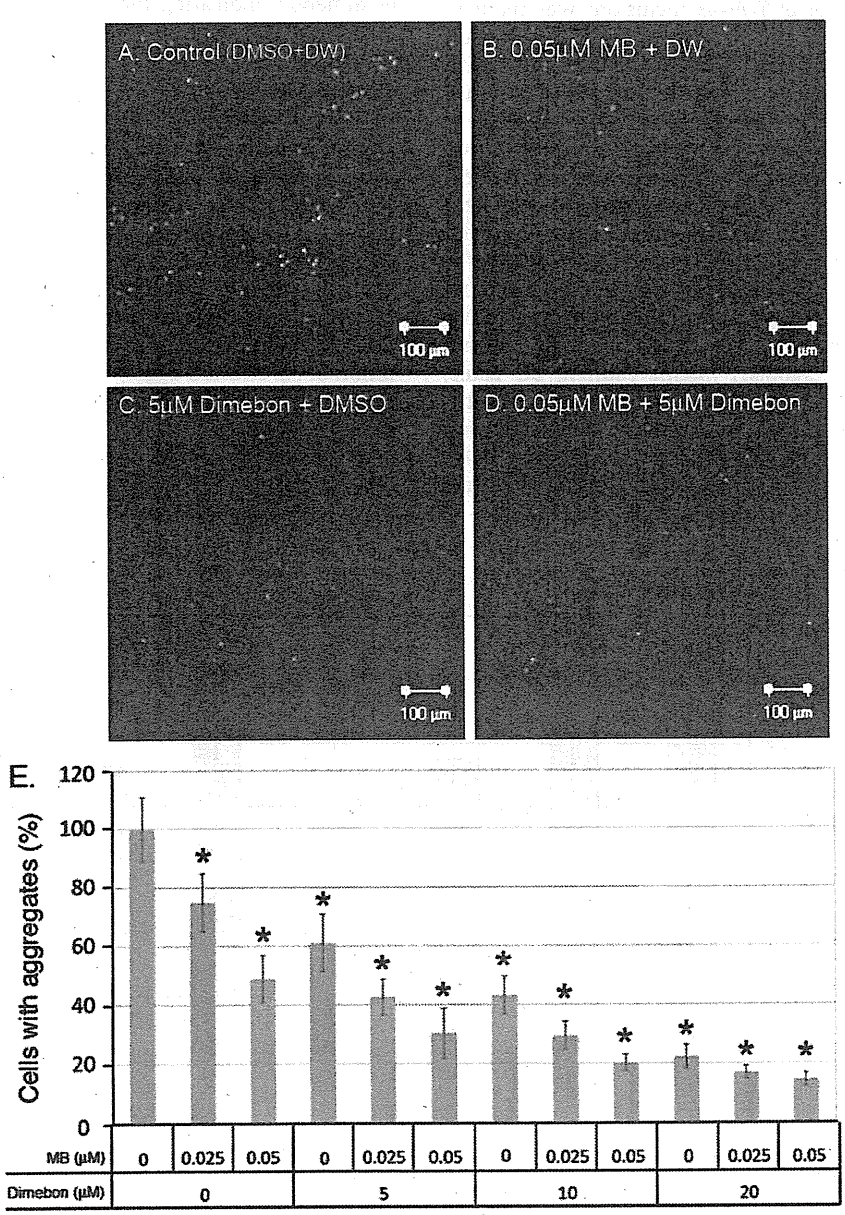

Fig. 2. Immunohistochemical analysis of the effects of methylene blue (MB) and dimebon on the aggregation of TDP-43 in SH-SY5Y cells expressing TDP-43 C-terminal fragment (162–414) as GFP fusion protein. TDP-43 inclusions were detected by fluorescence of GFP, when the laser power was adjusted. Representative confocal images from cells treated with control (DMSO + DW) (A), 0.05 μM MB + DW (B), 5 μM dimebon + DMSO (C) and 0.05 μM MB + 5 μM dimebon (D) are shown. (E) Quantitation of cells with TDP-43 aggregates. The intensity of fluorescence of GFP was calculated as the ratio of that of TOPRO-3. At least 8 areas per sample were measured (n = 8–16). Data are means ± S.E.M. $^{*}P < 0.01$ by Student's t test.

run on SDS–PAGE and immunoblotted with anti-TDP-43 and anti-pS409/410 antibodies, as described [33].

3. Results

3.1. Effects of MB and dimebon on the formation of TDP-43 inclusions

We first investigated the cytotoxicity of MB and dimebon. SH-SY5Y cells were treated with different concentrations of each compound, cultured for 1 day, followed by growth measurements. No toxic effects were detected with dimebon at concentrations of 1–60 μM, whereas a significant decrease in the number of cells was observed with MB at concentrations greater than 0.1 μM. Cells transfected with TDP-43 (ΔNLS&187-192) formed round intracellular inclusion-like structures that were positive with both anti-pS409/410 and anti-Ub antibodies, as reported previously [33] (Fig. 1A). When the cells were treated for 3 days with MB, dimebon or MB + dimebon, the number of TDP-43 inclusions was reduced (Fig. 1B–D). Compared to controls, we observed a 50% reduction in the number of inclusions with 0.05 μM MB, a 45% reduction with 5 μM dimebon and a 80% reduction with 0.05 μM MB + 5 μM dimebon (Fig. 1B–E). The effects were concentration-dependent and statistically significant (Fig. 1E). Thus, 10 μM dimebon caused a 60% reduction and 20 μM dimebon a 70% reduction in the number of TDP-43 inclusions. Similar results were obtained using a second cellular model of TDP-43 proteinopathy (Fig. 2), which expresses a C-terminal fragment (162–414) of TDP-43 as GFP fusion protein [34]. Other anti-histaminergic compounds, including promethazine hydrochloride, diphenhydramine hydrochloride (H1 histamine receptor antagonist) and thioperamide maleate (H3 histamine receptor antagonist) (Sigma–Aldrich, St. Louis, USA), did not affect the number of TDP-43 aggregates (Fig. 3). Similarly, two phenothiazine compounds tested, chlorpromazine hydrochloride and perphenazine (Sigma–Aldrich, St. Louis, USA), which failed to exert any effect on tau aggregation, did not affect the aggregation of TDP-43 (Fig. 3)

3.2. Immunoblot analysis of TDP-43 in cells treated with MB and dimebon

The immunohistochemical results were confirmed by immunoblotting. Cells expressing TDP-43 (ΔNLS&187-192) (data not shown) or the C-terminal fragment (162–414) of TDP-43 (Fig. 4) were sequentially extracted with TS, TX, and Sar, and the supernatants and pellets analyzed by immunoblotting. In cells transfected with the C-terminal fragment (162–414) of TDP-43, phosphorylated C-terminal fragment of TDP-43 was detected in the Sar-insoluble fraction, as reported previously [34] (black arrowhead in Fig 4A). The levels of this band with slower gel mobility were reduced when the cells were treated with MB, dimebon or MB + dimebon (Fig. 4A and B). By contrast, similar levels of endogenous TDP-43 (black arrow in Fig. 4A) and expressed C-terminal fragment of TDP-43 (white arrowhead in Fig. 4A) were detected in TS- and TX-soluble fractions of control cells and of cells treated with MB or dimebon, indicating that these compounds did not affect the amount of TDP-43.

4. Discussion

In this study, we examined the effects of two compounds, MB and dimebon, on the formation of abnormally phosphorylated TDP-43 inclusions using SH-SY5Y cellular models. Both compounds, when used singly or in combination, significantly reduced the number of TDP-43 aggregates. Although its mechanism of action remains to be clarified, it is reasonable to speculate that MB may bind to dimers and oligomers of TDP-43 and thereby inhibit fibril formation, as has previously been demonstrated for the inhibition of Aβ and tau aggregation by MB in vitro [27]. The present findings show, for the first time, that MB can reduce protein aggregation in cells.

In addition, we have identified dimebon as a compound capable of inhibiting the formation of abnormal inclusions of TDP-43. In view of the recent demonstration of its efficacy in a phase II

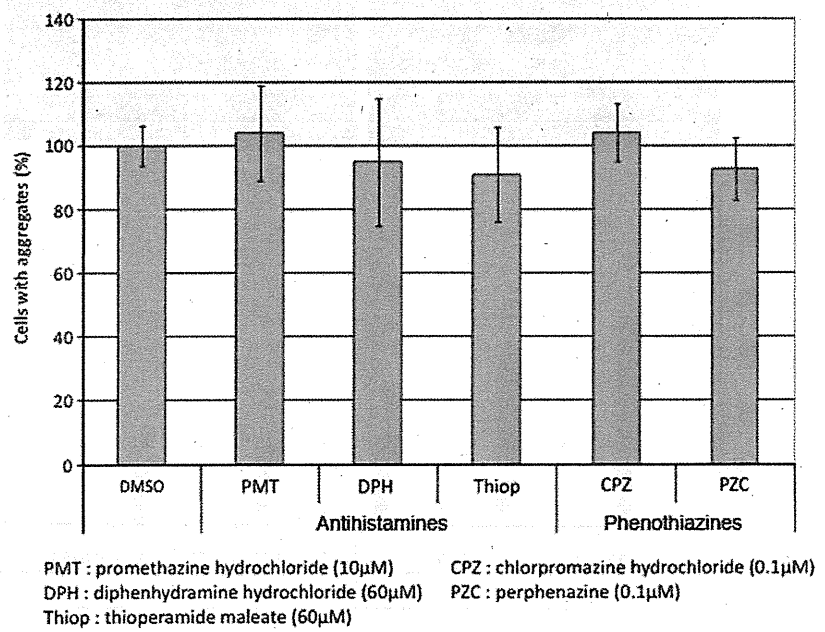

Fig. 3. Immunohistochemical analysis of the effects of three anti-histaminergic compounds, promethazine hydrochloride (PMT), diphenhydramine hydrochloride (DPH) and thioperamide maleate (Thiop), and two phenothiazine compounds, chlorpromazine hydrochloride (CPZ) and perphenazine (PZC) on the aggregation of TDP-43 in SH-SY5Y cells expressing GFP-fused TDP-43 C-terminal fragment (162–414) as GFP fusion protein. Quantitation of cells with TDP-43 aggregates is shown. No reduction in the TDP-43 aggregation was observed with these compounds. Promethazine hydrochloride and phenothiazines were tested at 10 μM and 0.1 μM, respectively, because they were toxic at higher concentrations.

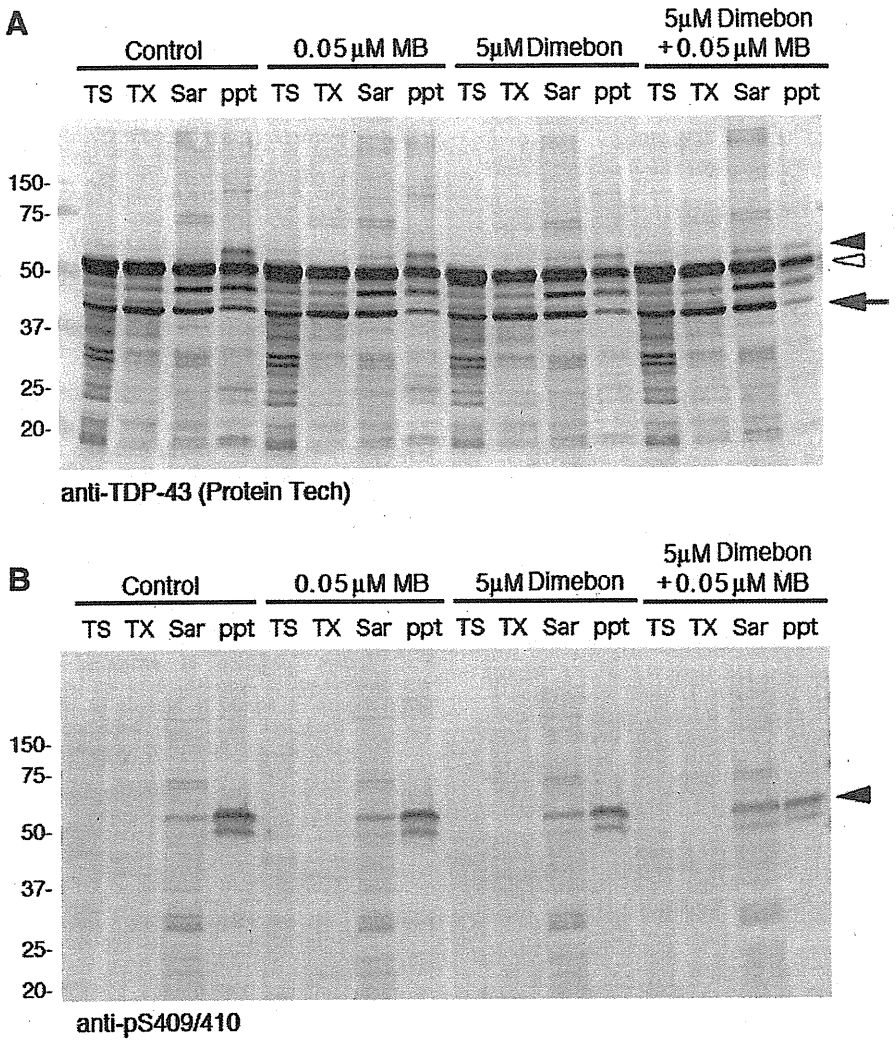

Fig. 4. Immunoblot analysis of the effects of methylene blue (MB) and dimebon on the aggregation of TDP-43 in SH-SY5Y cells expressing GFP-tagged TDP-43 C-terminal fragment (162–414). Tris saline (TS)-soluble material, Triton X-100 (TX)-soluble material, Sarkosyl (Sar)-soluble material and the remaining pellet (ppt) were prepared from control cells and from cells treated with 0.05 μM MB, 5 μM dimebon or 0.05 μM MB + 5 μM dimebon, run on SDS–PAGE and immunoblotted with anti-TDP-43 antibody (A) or anti-pS409/410 antibody (B). Abnormally phosphorylated TDP-43 C-terminal fragment (162–414) with a higher apparent molecular mass than the corresponding non-phosphorylated fragment (white arrowhead) was detected by both antibodies (black arrowheads). Similar levels of the non-phosphorylated GFP-tagged C-terminal fragment of TDP-43 (white arrowhead) and of endogenous TDP-43 (black arrow) were detected with the anti-TDP-43 antibody (A).

clinical trial, dimebon may well become a new drug for the treatment of AD and other neurodegenerative diseases. Although there have been some reports suggesting that dimebon may act as a neuroprotective agent and prevent mitochondrial pore transition in experimental models of AD [36] and Huntington's disease [30], its precise mode of action remains unknown. The present study suggests that dimebon may act by reducing the production or accumulation of abnormal protein aggregates. It remains to be determined whether the effects on TDP-43 aggregation are of a direct or an indirect nature. It will also be interesting to investigate the effects of dimebon in existing [37] and future animal models of TDP-43 proteinopathy. We could not detect a significant effect of dimebon on the in vitro assembly of recombinant human α-synuclein into filaments and on the heparin-induced assembly of recombinant human tau into filaments (data not shown). The recent demonstration that dimebon reduces the number of protein inclusions in a model synucleinopathy [32] suggests that its effects may be indirect.

MB has been used for many years to treat a variety of conditions, including methemoglobinemia [19], septic shock [20] and depression [38]. It has recently been used in a phase II trial of AD [16]. Furthermore, MB has been reported to have activity as an enhancer of mitochondrial activity [24], and a recent study has reported that it delays cellular senescence in cultured human fibroblasts [25]. However, high doses of MB are known to be toxic and to cause the formation of Heinz bodies in erythrocytes in infants [39]. A combination therapy, like the one used here, may therefore be advantageous.

In conclusion, the present results showing a reduction in the number of TDP-43 inclusions following the addition of MB and/or dimebon to transfected SH-SY5Y cells suggest that these compounds may be beneficial for the treatment of ALS and FTLD-U.

Acknowledgements

We thank Dr. Shahin Zibaee for helpful comments on the manuscript. This work was supported by a Grant-in-aid for Scientific Research on Priority Area – Research on Pathomechanisms of Brain Disorders (to M.H., 20023038) from Ministry of Education, Culture, Sports, Science and Technology and grants from Ministry of Health, Labor and Welfare of Japan, and a Russian Foundation for Basic Research Grant (to N.N., 09-04-01412-a).

References

[1] Neumann, M., Sampathu, D.M., Kwong, L.K., Truax, A.C., Micsenyi, M.C., Chou, T.T., Bruce, J., Schuck, T., Grossman, M., Clark, C.M., McCluskey, L.F., Miller, B.L., Masliah, E., Mackenzie, I.R., Feldman, H., Feiden, W., Kretzschmar, H.A., Trojanowski, J.Q. and Lee, V.M. (2006) Ubiquitinated TDP-43 in frontotemporal lobar degeneration and amyotrophic lateral sclerosis. Science 314, 130–133.

[2] Arai, T., Hasegawa, M., Akiyama, H., Ikeda, K., Nonaka, T., Mori, H., Mann, D., Tsuchiya, K., Yoshida, M., Hashizume, Y. and Oda, T. (2006) TDP-43 is a component of ubiquitin-positive tau-negative inclusions in frontotemporal lobar degeneration and amyotrophic lateral sclerosis. Biochem. Biophys. Res. Commun. 351, 602–611.

[3] Davidson, Y., Kelley, T., Mackenzie, I.R., Pickering-Brown, S., Du Plessis, D., Neary, D., Snowden, J.S. and Mann, D.M. (2007) Ubiquitinated pathological lesions in frontotemporal lobar degeneration contain the TAR DNA-binding protein. TDP-43. Acta Neuropathol. 113, 521–533.

[4] Hasegawa, M., Arai, T., Nonaka, T., Kametani, F., Yoshida, M., Hashizume, Y., Beach, T.G., Buratti, E., Baralle, F., Morita, M., Nakano, I., Oda, T., Tsuchiya, K. and Akiyama, H. (2008) Phosphorylated TDP-43 in frontotemporal lobar degeneration and amyotrophic lateral sclerosis. Ann. Neurol. 64, 60–70.

[5] Yokoseki, A., Shiga, A., Tan, C.F., Tagawa, A., Kaneko, H., Koyama, A., Eguchi, H., Tsujino, A., Ikeuchi, T., Kakita, A., Okamoto, K., Nishizawa, M., Takahashi, H. and Onodera, O. (2008) TDP-43 mutation in familial amyotrophic lateral sclerosis. Ann. Neurol. 63, 538–542.

[6] Sreedharan, J., Blair, I.P., Tripathi, V.B., Hu, X., Vance, C., Rogelj, B., Ackerley, S., Durnall, J.C., Williams, K.L., Buratti, E., Baralle, F., de Belleroche, J., Mitchell, J.D., Leigh, P.N., Al-Chalabi, A., Miller, C.C., Nicholson, G. and Shaw, C.E. (2008) TDP-43 mutations in familial and sporadic amyotrophic lateral sclerosis. Science 319, 1668–1672.

[7] Rutherford, N.J., Zhang, Y.J., Baker, M., Gass, J.M., Finch, N.A., Xu, Y.F., Stewart, H., Kelley, B.J., Kuntz, K., Crook, R.J., Sreedharan, J., Vance, C., Sorenson, E., Lippa, C., Bigio, E.H., Geschwind, D.H., Knopman, D.S., Mitsumoto, H., Petersen, R.C., Cashman, N.R., Hutton, M., Shaw, C.E., Boylan, K.B., Boeve, B., Graff-Radford, N.R., Wszolek, Z.K., Caselli, R.J., Dickson, D.W., Mackenzie, I.R., Petrucelli, L. and Rademakers, R. (2008) Novel mutations in TARDBP (TDP-43) in patients with familial amyotrophic lateral sclerosis. PLoS Genet. 4, e1000193.

[8] Kabashi, E., Valdmanis, P.N., Dion, P., Spiegelman, D., McConkey, B.J., Vande Velde, C., Bouchard, J.P., Lacomblez, L., Pochigaeva, K., Salachas, F., Pradat, P.F., Camu, W., Meininger, V., Dupre, N. and Rouleau, G.A. (2008) TARDBP mutations in individuals with sporadic and familial amyotrophic lateral sclerosis. Nat. Genet. 40, 572–574.

[9] Gitcho, M.A., Baloh, R.H., Chakraverty, S., Mayo, K., Norton, J.B., Levitch, D., Hatanpaa, K.J., White 3rd, C.L., Bigio, E.H., Caselli, R., Baker, M., Al-Lozi, M.T., Morris, J.C., Pestronk, A., Rademakers, R., Goate, A.M. and Cairns, N.J. (2008) TDP-43 A315T mutation in familial motor neuron disease. Ann. Neurol. 63, 535–538.

[10] Arai, T., Mackenzie, I.R., Hasegawa, M., Nonoka, T., Niizato, K., Tsuchiya, K., Iritani, S., Onaya, M. and Akiyama, H. (2009) Phosphorylated TDP-43 in Alzheimer's disease and dementia with Lewy bodies. Acta Neuropathol. 117, 125–136.

[11] Hasegawa, M., Arai, T., Akiyama, H., Nonaka, T., Mori, H., Hashimoto, T., Yamazaki, M. and Oyanagi, K. (2007) TDP-43 is deposited in the Guam parkinsonism-dementia complex brains. Brain 130, 1386–1394.

[12] Fujishiro, H., Uchikado, H., Arai, T., Hasegawa, M., Akiyama, H., Yokota, O., Tsuchiya, K., Togo, T., Iseki, E. and Hirayasu, Y. (2009) Accumulation of phosphorylated TDP-43 in brains of patients with argyrophilic grain disease. Acta Neuropathol. 117, 151–158.

[13] Schwab, C., Arai, T., Hasegawa, M., Yu, S. and McGeer, P.L. (2008) Colocalization of transactivation-responsive DNA-binding protein 43 and huntingtin in inclusions of huntington disease. J. Neuropathol. Exp. Neurol. 67, 1159–1165.

[14] Farrer, M.J., Hulihan, M.M., Kachergus, J.M., Dachsel, J.C., Stoessl, A.J., Grantier, L.L., Calne, S., Calne, D.B., Lechevalier, B., Chapon, F., Tsuboi, Y., Yamada, T., Gutmann, L., Elibol, B., Bhatia, K.P., Wider, C., Vilarino-Guell, C., Ross, O.A., Brown, L.A., Castanedes-Casey, M., Dickson, D.W. and Wszolek, Z.K. (2009) DCTN1 mutations in Perry syndrome. Nat. Genet. 41, 163–165.

[15] Schwab, C., Arai, T., Hasegawa, M., Akiyama, H., Yu, S. and McGeer, P.L. (2009) TDP-43 pathology in familial British dementia. Acta Neuropathol., in press, doi:10.1007/s00401-009-0514-3.

[16] Gura, T. (2008) Hope in Alzheimer's fight emerges from unexpected places. Nat. Med. 14, 894.

[17] Doody, R.S., Gavrilova, S.I., Sano, M., Thomas, R.G., Aisen, P.S., Bachurin, S.O., Seely, L. and Hung, D. (2008) Effect of dimebon on cognition, activities of daily living, behaviour, and global function in patients with mild-to-moderate Alzheimer's disease: a randomised, double-blind, placebo-controlled study. Lancet 372, 207–215.

[18] Kristiansen, J.E. (1989) Dyes, antipsychotic drugs, and antimicrobial activity. Fragments of a development, with special reference to the influence of Paul Ehrlich. Dan Med. Bull. 36, 178–185.

[19] Mansouri, A. and Lurie, A.A. (1993) Concise review: methemoglobinemia. Am. J. Hematol. 42, 7–12.

[20] Faber, P., Ronald, A. and Millar, B.W. (2005) Methylthioninium chloride: pharmacology and clinical applications with special emphasis on nitric oxide mediated vasodilatory shock during cardiopulmonary bypass. Anaesthesia 60, 575–587.

[21] Heiberg, I.L., Wegener, G. and Rosenberg, R. (2002) Reduction of cGMP and nitric oxide has antidepressant-like effects in the forced swimming test in rats. Behav. Brain Res. 134, 479–484.

[22] Visarius, T.M., Stucki, J.W. and Lauterburg, B.H. (1997) Stimulation of respiration by methylene blue in rat liver mitochondria. FEBS Lett. 412, 157–160.

[23] Chies, A.B., Custodio, R.C., de Souza, G.L., Correa, F.M. and Pereira, O.C. (2003) Pharmacological evidence that methylene blue inhibits noradrenaline neuronal uptake in the rat vas deferens. Pol. J. Pharmacol. 55, 573–579.

[24] Wrubel, K.M., Riha, P.D., Maldonado, M.A., McCollum, D. and Gonzalez-Lima, F. (2007) The brain metabolic enhancer methylene blue improves discrimination learning in rats. Pharmacol. Biochem. Behav. 86, 712–717.

[25] Atamna, H., Nguyen, A., Schultz, C., Boyle, K., Newberry, J., Kato, H. and Ames, B.N. (2008) Methylene blue delays cellular senescence and enhances key mitochondrial biochemical pathways. FASEB J. 22, 703–712.

[26] Wischik, C.M., Edwards, P.C., Lai, R.Y., Roth, M. and Harrington, C.R. (1996) Selective inhibition of Alzheimer disease-like tau aggregation by phenothiazines. Proc. Natl. Acad. Sci. USA 93, 11213–11218.

[27] Taniguchi, S., Suzuki, N., Masuda, M., Hisanaga, S., Iwatsubo, T., Goedert, M. and Hasegawa, M. (2005) Inhibition of heparin-induced tau filament formation by phenothiazines, polyphenols, and porphyrins. J. Biol. Chem. 280, 7614–7623.

[28] Burns, A. and Jacoby, R. (2008) Dimebon in Alzheimer's disease: old drug for new indication. Lancet 372, 179–180.

[29] Bachurin, S., Bukatina, E., Lermontova, N., Tkachenko, S., Afanasiev, A., Grigoriev, V., Grigorieva, I., Ivanov, Y., Sablin, S. and Zefirov, N. (2001) Antihistamine agent Dimebon as a novel neuroprotector and a cognition enhancer. Ann. NY Acad. Sci. 939, 425–435.

[30] Wu, J., Li, Q. and Bezprozvanny, I. (2008) Evaluation of dimebon in cellular model of Huntington's disease. Mol. Neurodegener. 3, 15.

[31] Lermontova, N.N., Redkozubov, A.E., Shevtsova, E.F., Serkova, T.P., Kireeva, E.G. and Bachurin, S.O. (2001) Dimebon and tacrine inhibit neurotoxic action of beta-amyloid in culture and block L-type Ca(2+) channels. Bull. Exp. Biol. Med. 132, 1079–1083.

[32] Bahurin, S.O., Ustyugov, A.A., Peters, O., Shelkovnikova, T.A., Buchman, V.L. and Ninkina, N.N. (2009). Hindering of proteinopathy-induced neurodegeneration as a new mechanism of action for neuroprotectors and cognition enhancing compounds. Dokl. Biochem. Biophys., in press.

[33] Nonaka, T., Arai, T., Buratti, E., Baralle, F.E., Akiyama, H. and Hasegawa, M. (2009) Phosphorylated and ubiquitinated TDP-43 pathological inclusions in ALS and FTLD-U are recapitulated in SH-SY5Y cells. FEBS Lett. 583, 394–400.

[34] Nonaka, T., Kametani, F., Arai, T., Akiyama, H. and Hasegawa, M. (2009). Truncation and pathogenic mutations facilitate the formation of intracellular aggregates of TDP-43. Hum. Mol. Genet., in press, doi:10.1093/hmg/ddp275.

[35] Johnson, B.S., McCaffery, J.M., Lindquist, S. and Gitler, A.D. (2008) A yeast TDP-43 proteinopathy model: exploring the molecular determinants of TDP-43 aggregation and cellular toxicity. Proc. Natl. Acad. Sci. USA 105, 6439–6444.

[36] Lermontova, N.N., Lukoyanov, N.V., Serkova, T.P., Lukoyanova, E.A. and Bachurin, S.O. (2000) Dimebon improves learning in animals with experimental Alzheimer's disease. Bull. Exp. Biol. Med. 129, 544–546.

[37] Tatom, J.B., Wang, D.B., Dayton, R.D., Skalli, O., Hutton, M.L., Dickson, D.W. and Klein, R.L. (2009) Mimicking aspects of frontotemporal lobar degeneration and Lou Gehrig's disease in rats via TDP-43 overexpression. Mol. Ther. 17, 607–613.

[38] Naylor, G.J., Martin, B., Hopwood, S.E. and Watson, Y. (1986) A two-year double-blind crossover trial of the prophylactic effect of methylene blue in manic-depressive psychosis. Biol. Psychiatr. 21, 915–920.

[39] Sills, M.R. and Zinkham, W.H. (1994) Methylene blue-induced Heinz body hemolytic anemia. Arch Pediatr. Adolesc. Med. 148, 306–310.

Human Molecular Genetics, 2009, Vol. 18, No. 18 **3353–3364**
doi:10.1093/hmg/ddp275
Advance Access published on June 10, 2009

Truncation and pathogenic mutations facilitate the formation of intracellular aggregates of TDP-43

Takashi Nonaka[1,*], Fuyuki Kametani[1], Tetsuaki Arai[2], Haruhiko Akiyama[2] and Masato Hasegawa[1,*]

[1]Department of Molecular Neurobiology and [2]Department of Psychogeriatrics, Tokyo Institute of Psychiatry, Tokyo Metropolitan Organization for Medical Research, 2-1-8 Kamikitazawa, Setagaya-ku, Tokyo 156-8585, Japan

Received April 5, 2009; Revised May 27, 2009; Accepted June 8, 2009

TAR DNA binding protein of 43 kDa (TDP-43) is a major component of the ubiquitin-positive inclusions found in the brain of patients with frontotemporal lobar degeneration (FTLD-U) and amyotrophic lateral sclerosis (ALS). Here, we report that expression of TDP-43 C-terminal fragments as green fluorescent protein (GFP) fusions in SH-SY5Y cells results in the formation of abnormally phosphorylated and ubiquitinated inclusions that are similar to those found in FTLD-U and ALS. Co-expression of DsRed-tagged full-length TDP-43 with GFP-tagged C-terminal fragments of TDP-43 causes formation of cytoplasmic inclusions positive for both GFP and DsRed. Cells with GFP and DsRed positive inclusions lack normal nuclear staining for endogenous TDP-43. These results suggest that GFP-tagged C-terminal fragments of TDP-43 are bound not only to transfected DsRed-full-length TDP-43 but also to endogenous TDP-43. Endogenous TDP-43 may be recruited to cytoplasmic aggregates of TDP-43 C-terminal fragments, which results in the failure of its nuclear localization and function. Interestingly, expression of GFP-tagged TDP-43 C-terminal fragments harboring pathogenic mutations that cause ALS significantly enhances the formation of inclusions. We also identified cleavage sites of TDP-43 C-terminal fragments deposited in the FTLD-U brains using mass spectrometric analyses. We propose that generation and aggregation of phosphorylated C-terminal fragments of TDP-43 play a primary role in the formation of inclusions and resultant loss of normal TDP-43 localization, leading to neuronal degeneration in TDP-43 proteinopathy.

INTRODUCTION

Progressive neuronal loss and abnormal protein deposits as intracellular inclusions are neuropathological features of the majority of neurodegenerative disorders, as exemplified by tau in Alzheimer's disease (AD), alpha-synuclein in Parkinson's disease (PD) and expanded polyglutamine gene products in CAG repeat diseases. Conformational changes, post-translational modifications or subcellular mislocalization of these normally highly soluble proteins results in the formation of abnormal protein aggregates or inclusions. It is important to establish the molecular mechanisms through which these proteins are converted to abnormal aggregates in neurons or glial cells in order to understand the pathogenesis of these diseases and to develop evidence-based, fundamental therapies.

Frontotemporal lobar degeneration with ubiquitinated inclusions (FTLD-U) and amyotrophic lateral sclerosis (ALS) are well-known neurodegenerative disorders. FTLD is the second most common form of cortical dementia in the population below the age of 65 years (1). ALS is the most common of the motor neuron diseases, being characterized by progressive weakness and muscular wasting, resulting in death within a few years. Ubiquitin (Ub)-positive inclusions are found as a pathological hallmark in brains of FTLD-U and ALS patients, as well as in AD and PD, but the major component of these inclusions had remained unknown. TAR-DNA binding protein of 43 kDa (TDP-43) has been identified as a major protein component of Ub-positive inclusions in FTLD-U and ALS brains (2,3). In 2008, mutations in the TDP-43 gene were discovered in familial

*To whom correspondence should be addressed. Tel: +81 333045701; Fax: +81 333298035; Email: nonakat@prit.go.jp (T.N.)/masato@prit.go.jp (M.H.)

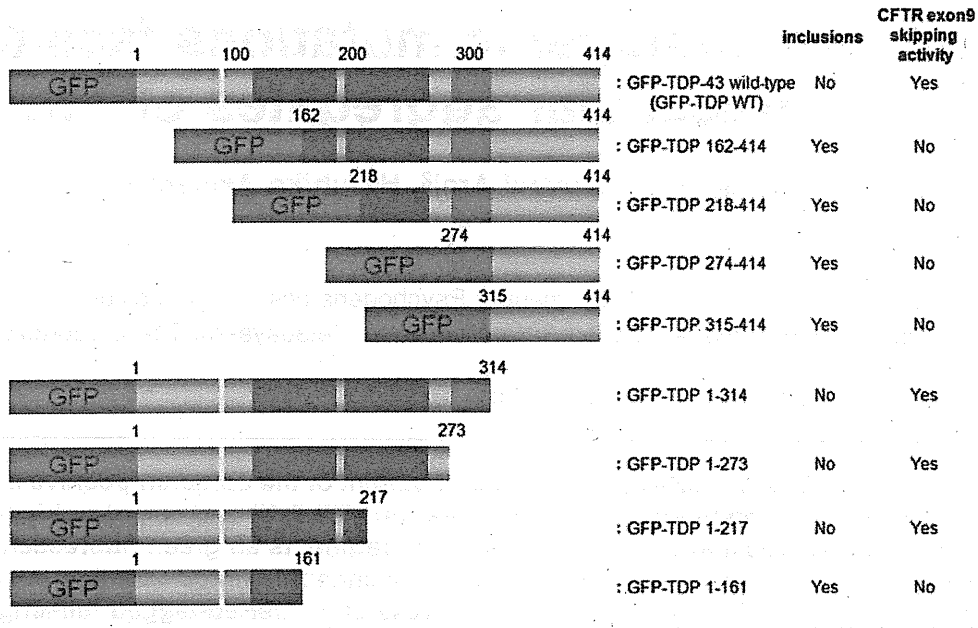

Figure 1. Schematic diagram of GFP-tagged N-terminal and C-terminal TDP-43 fragments. Green fluorescent protein (GFP), nuclear localization signal (NLS: 82–98 residues), two RNA-recognition motifs (RRM-1, 105–169 residues; RRM-2, 193–257 residues) and glycine-rich domain (274–314 residues) were colored green, yellow, blue and red, respectively. The formation of inclusions and the exon skipping ability of each fragment were reported on the right. The CFTR exon 9 skipping activity of these fragments were determined as shown in Fig. 5.

and sporadic cases of ALS (4–8), clearly indicating that abnormality of TDP-43 protein causes neurodegeneration. Very recently, it was also reported that two TDP-43 mutations were found in FTLD-MND patients (9). In previous genetic studies of familial ALS, superoxide dismutase 1 (SOD1) gene mutation was considered to be responsible for ~20% of cases (10,11). It has been reported, however, that TDP-43 is not deposited in spinal cords of familial ALS patients with SOD1 mutations (12,13). These observations suggest that the mechanisms of motor neuron degeneration caused by SOD1 mutations are different from those in sporadic ALS. TDP-43 is also a major component of skein-like inclusions seen in 100% of sporadic ALS cases (14). Thus, it is important to investigate the molecular mechanisms of TDP-43-mediated neurodegeneration in order to understand the pathogenesis and to develop effective treatments for sporadic ALS and other TDP-43 proteinopathies. One of the known biochemical features of TDP-43 deposited in FTLD-U and ALS brains is the presence of truncated TDP-43 fragments (2,3). Recently, using multiple anti-phosphorylated TDP-43 specific antibodies including pS409/410-specific antibodies, we have shown that 18–26 kDa C-terminal fragments of TDP-43 are major constituents of inclusions in FTLD-U and ALS brains (15).

In this study, we investigated the roles of fragmentation and pathogenic mutations of TDP-43 for the formation of Ub-positive inclusions in SH-SY5Y cells. Here we show that expression of TDP-43 C-terminal fragments results in the formation of cytoplasmic inclusions positive for antibodies to phosphorylated TDP-43 and Ub, and incorporation of newly synthesized endogenous full-length TDP-43 into cytoplasmic aggregates of the C-terminal fragments. Expression of fourteen pathogenic ALS mutations so far discovered in the TDP-43 gene shows a propensity to promote intracellular aggregation. Furthermore, using mass spectrometric analysis, we have successfully identified new cleavage sites of C-terminal fragments of TDP-43 deposited in FTLD-U brains.

RESULTS

Expression of TDP-43 fragments in SH-SY5Y cells

To examine whether C-terminal fragments of TDP-43 readily aggregate in neuronal cells, we expressed several kinds of N-terminal and C-terminal fragments of TDP-43 and full-length TDP-43 as GFP-fusions (Fig. 1). Confocal microscopic analysis showed that the fluorescence of GFP-tagged full-length TDP-43 (GFP-TDP WT) was mainly localized in the nuclei (Fig. 2B). This is consistent with the expression pattern of non-tagged wild-type TDP-43 (16), suggesting that the GFP tag did not alter the cellular localization of TDP-43.

When cells were transfected with GFP-TDP 162-414 or GFP-TDP 218-414, round or dot-like cytoplasmic structures with intense GFP fluorescence were found (Fig. 2C–F). These structures were positive for both anti-pS409/410 and anti-Ub antibodies (Fig. 2C–F). Cells expressing GFP-TDP 274–414 (Fig. 2G and H) and GFP-TDP 315–414 (Fig. 2I and J), on the other hand, showed diffuse GFP staining and pS409/410-positive but Ub-negative inclusion-like structures. We previously reported the presence of such pS409/410-positive and Ub-negative inclusions in the brains of FTLD-U and ALS cases (15). The expression of these all C-terminal fragments was found in cytoplasm by analyses using confocal microscopy (Fig. 2) and biochemical fractionation (Supplementary Material, Fig. S1A), because they lacks nuclear localization signal (16,17). Taken together, these results indicate that cytoplasmic expression of C-terminal

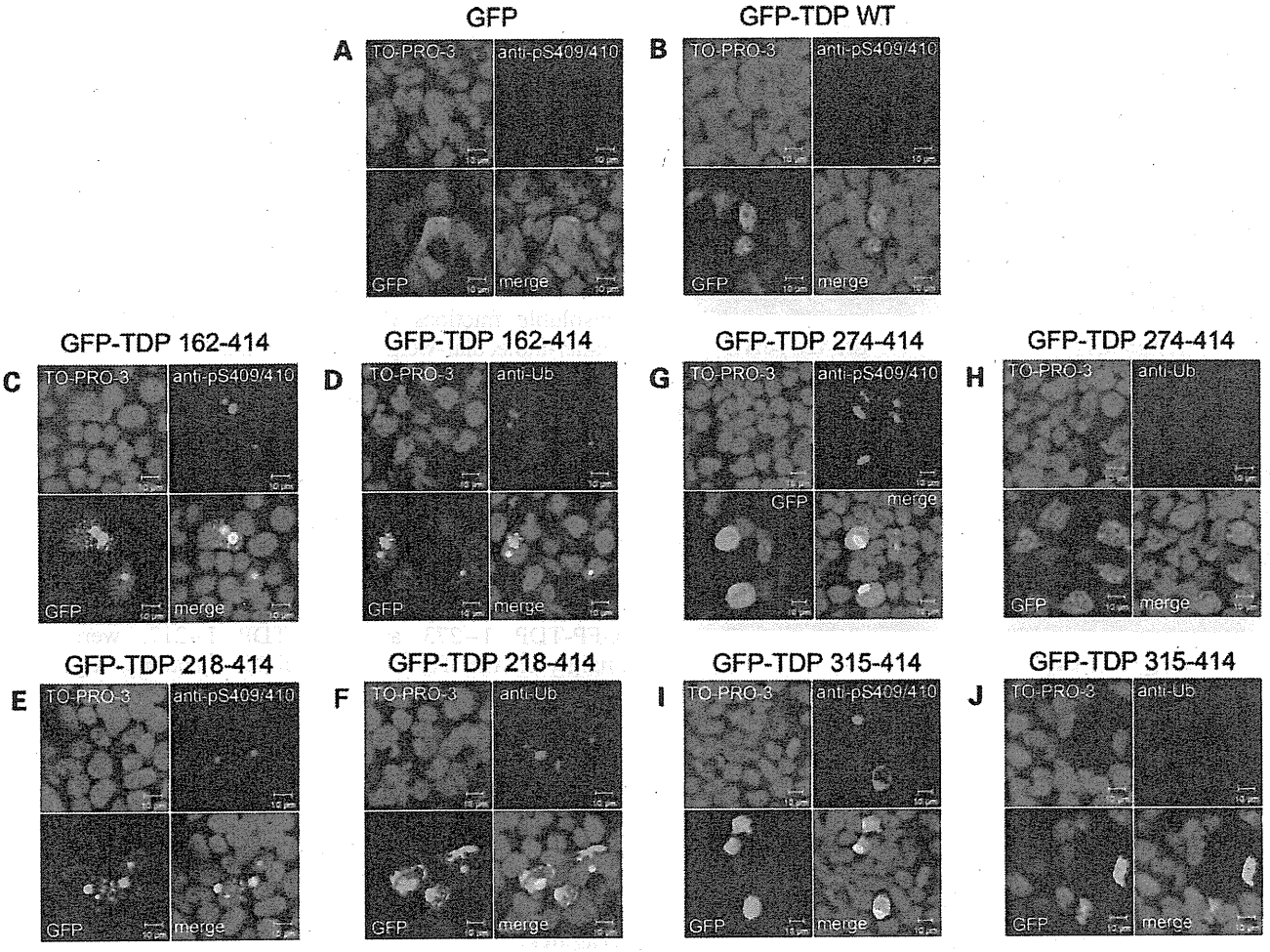

Figure 2. Expression of GFP-tagged C-terminal fragments of TDP-43 leads to aggregate formation in SH-SY5Y cells. SH-SY5Y cells 72 h post-transfection with GFP (**A**), GFP-tagged TDP-43 wild-type (GFP-TDP WT) (**B**), GFP-tagged fragments of residues 162–414 (GFP-TDP 162–414) (**C** and **D**), GFP-TDP 218–414 (**E** and **F**), GFP-TDP 274–414 (**G** and **H**) and GFP-TDP 315–414 (**I** and **J**) were stained with anti-pS409/410 (A, B, C, E, G, I) or anti-Ub (D, F, H, J). DNA was labeled with TO-PRO-3. Note that there are intracellular inclusion-like structures positive for both anti-Ub and anti-pS409/410 antibodies in cells expressing GFP-TDP 162–414 (C, D) and GFP-TDP 218–414 (E, F).

fragments of TDP-43 results in the formation of intracellular aggregates similar to those found in diseased brains.

N-terminal fragments of GFP-TDP-43 were also expressed in SH-SY5Y cells and analyzed using confocal microscopy and biochemical fractionation. As shown in Fig. 3A, irregularly shaped cytoplasmic structures with strong GFP fluorescence, which are partially positive for Ub, were observed in cells expressing GFP-TDP 1–161. Only a few aggregates positive for Ub were observed in cells transfected with GFP-TDP 1–217 (Fig. 3B). Since these fragments lack the epitope for anti-pS409/410, the phosphorylation state of these structures could not be determined by immunohistochemistry. None of the cells transfected with other N-terminal fragments had any Ub-positive inclusion-like structures (Fig. 3C and D). The results of biochemical fractionation showed that the amount of these N-terminal fragments was greater in the cytoplasm than in the nucleus, while that of GFP-TDP WT was greater in the nucleus than in the cytoplasm (Supplementary Material, Fig. S1A). These results suggest that truncations of TDP-43 C-terminal regions affect normal targeting of TDP-43 to nuclei. This observation is in good agreement with the previous report by Ayala *et al.* (18).

Since intracellular inclusion-like structures showed the highest-intensity GFP signals in Figs 2 and 3, they were able to be selectively detected by reducing the laser power at 488 nm. Quantitative analyses under such analytical conditions clearly indicated that significantly a larger number of intracellular aggregates were formed in cells expressing GFP-TDP 162–414, GFP-TDP 218–414 and GFP-TDP 1–161 than in cells expressing GFP-TDP WT (Fig. 3E).

Figure 4 shows the results of immunoblot analyses of cell lysates using anti-GFP, a commercially available phosphorylation-independent anti-TDP-43 (ProteinTech), and anti-pS409/410 antibodies. Anti-TDP-43 detected endogenous TDP-43 at 43 kDa, exogenous full-length TDP-43, all N-terminal fragments and GFP-TDP 162–414, but did not GFP-TDP 218–414, 274–414 and 315–414 (Fig. 4A and D). These results suggest that the epitopes of this antibody are located in the N-terminal region between 1 and 217 residues. Anti-GFP antibody stained all the exogenous TDP-43

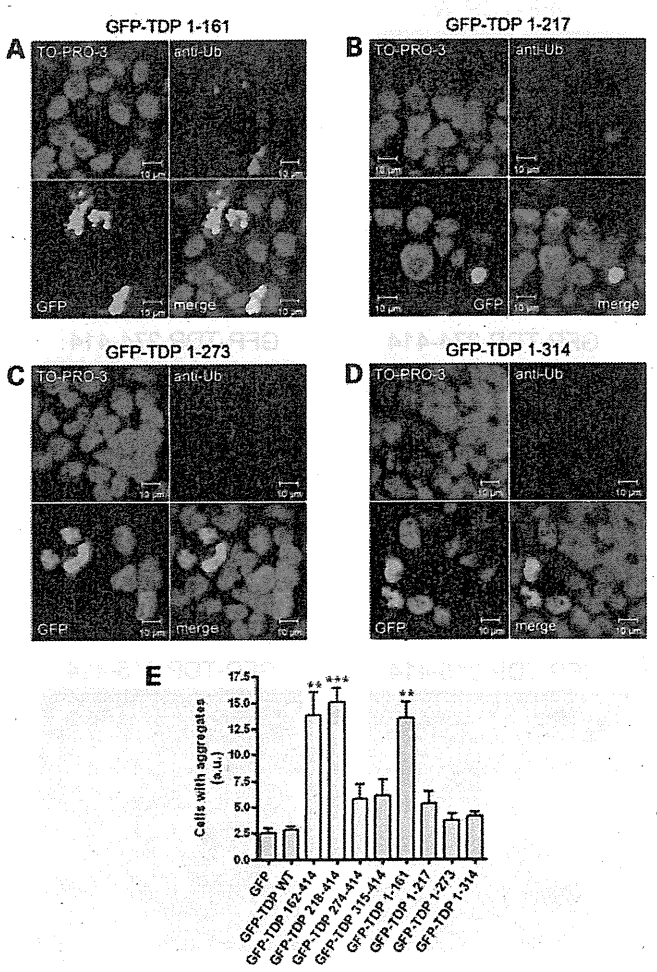

Figure 3. Expression of GFP-tagged N-terminal fragments of TDP-43 resulted in the formation of intracellular inclusions in SH-SY5Y cells. SH-SY5Y cells 72 h post-transfection with GFP-tagged fragments of 1–161 residues (GFP-TDP 1–161) (**A**), GFP-TDP 1–217 (**B**), GFP-TDP 1–273 (**C**) and GFP-TDP 1–314 (**D**) were stained with anti-Ub. DNA was labeled with TO-PRO-3. Note the characteristic inclusions detected with anti-Ub antibody in cells transfected with GFP-TDP 1–161. (**E**) The rates of cells including intracellular aggregates were calculated in arbitrary units. Fluorescence intensity within an area of ~800 × 800 μm was assessed by confocal microscopy. The intensity of GFP was calculated as a ratio to that of TO-PRO-3. Six areas per sample were measured ($n = 6$). Data are means ± SEM. $^{**}P < 0.01$; $^{***}P < 0.001$ by Student's *t*-test against the value of GFP-TDP WT.

(Fig. 4B and E). In these immunoblot analyses, we used the intensity of the bands of endogenous TDP-43 (arrows in Fig. 4A and D) as a loading control. While the amounts of exogenous protein are nearly constant, that of 1–161 is relatively low and those of 274–414 and 315–414 relatively high. Nevertheless, such variability does not affect the occurrence or absence of inclusion formation (Fig. 1). Endogenous and exogenous full-length TDP-43 (GFP-TDP WT) were detected mostly in TS-, TX- and Sar-soluble fractions, and were negative for anti-pS409/410 (Fig. 4).

Although GFP-TDP 162–414 was also detected in TS-, TX- and Sar-soluble fractions with anti-TDP-43 and anti-GFP, a slightly higher-molecular-weight band (~60 kDa, black arrowhead in Fig. 4C) was detected in Sar-soluble and insoluble fractions with anti-pS409/410. A similar band was only weakly detected with anti-TDP-43 (black arrowhead in Fig. 4A), and was negative to anti-GFP antibody. These results confirmed our previous reports that our anti-pS409/410 is specific to and is more sensitive in detecting abnormally accumulated TDP-43 than phosphorylation-independent antibodies such as anti-TDP-43 (ProteinTech) (15,16,19). Anti-GFP used here seems to be less sensitive in immunoblot. Anti-GFP may also be affected by possible structural changes during aggregates formation when applied to the Sarkosyl insoluble fraction. GFP-TDP 218–414 was mainly detected in Sar-soluble and -insoluble fractions with anti-GFP (Fig. 4B), and a slightly higher-molecular-weight band at 52 kDa (white arrowhead in Fig. 4C) and smears were visualized in the Sar-soluble and -insoluble fractions with anti-pS409/410. Similarly, pS409/410-positive bands were detected in the Sar-soluble and insoluble fractions of cell lysates expressing GFP-TDP 274–414 or GFP-TDP 315–414 (black-lined arrowhead for GFP-TDP-274–414; white-lined arrowhead for GFP-TDP 315–414 in Fig. 4C), although no abnormal band pattern was detected with anti-TDP-43 or anti-GFP.

The N-terminal fragments, including GFP-TDP 1–314, GFP-TDP 1–273 and GFP-TDP 1–217, were detected mainly in the TS- and TX-soluble fractions, together with GFP-TDP WT and endogenous TDP-43 (Fig. 4D and E). However, GFP-TDP 1–161, the shortest N-terminal fragment, was detected only in the Sar-soluble fraction (black-lined arrowheads in Fig. 4D and E), which is consistent with the inclusion formation observed in cells expressing this fragment, as shown in Fig. 3A.

Loss of function and intracellular accumulation of TDP-43 fragments

TDP-43 has been reported to regulate the alternative splicing of exon 9 of cystic fibrosis transmembrane conductance regulator (CFTR) transcripts (20). TDP-43 is capable of binding to a (UG)nUm element in CFTR intron 8 near its junction with exon 9. Through this binding, TDP-43 enhances the exon skipping of exon 9 during CFTR splicing. To evaluate the functional significance of TDP-43 fragments used in this study, we performed CFTR exon 9 skipping assay (16). We co-transfected the expression plasmid of TDP-43 wild-type or fragments with the reporter plasmid pSPL3-CFTR9 (including a TG11T7 polymorphic locus) (16) into SH-SY5Y cells. The transcripts with and without the CFTR exon 9 insert are expected to be 360 and 177 bp long, respectively (16), and these were analyzed by RT–PCR. As shown in Fig. 5, mRNA from cells transfected with empty vector pEGFP gave only one RT–PCR band of 360 bp, while that from cells transfected with TDP-43 wild-type gave two RT–PCR bands, 360 and 177 bp, showing that skipping of CFTR exon 9 was increased by expression of GFP-TDP WT. We also confirmed that the GFP portion did not affect the CFTR exon skipping activity of TDP-43. All mRNAs from cells co-transfected with the C-terminal fragments showed one RT–PCR band of 360 bp (Fig. 5A). Of the four mRNAs from cells co-transfected with the N-terminal fragments, mRNA from GFP-TDP 1-161 showed a band of 360 bp, while the others showed two bands of 360 and 177 bp (Fig. 5B). These results indicate that the fragments without

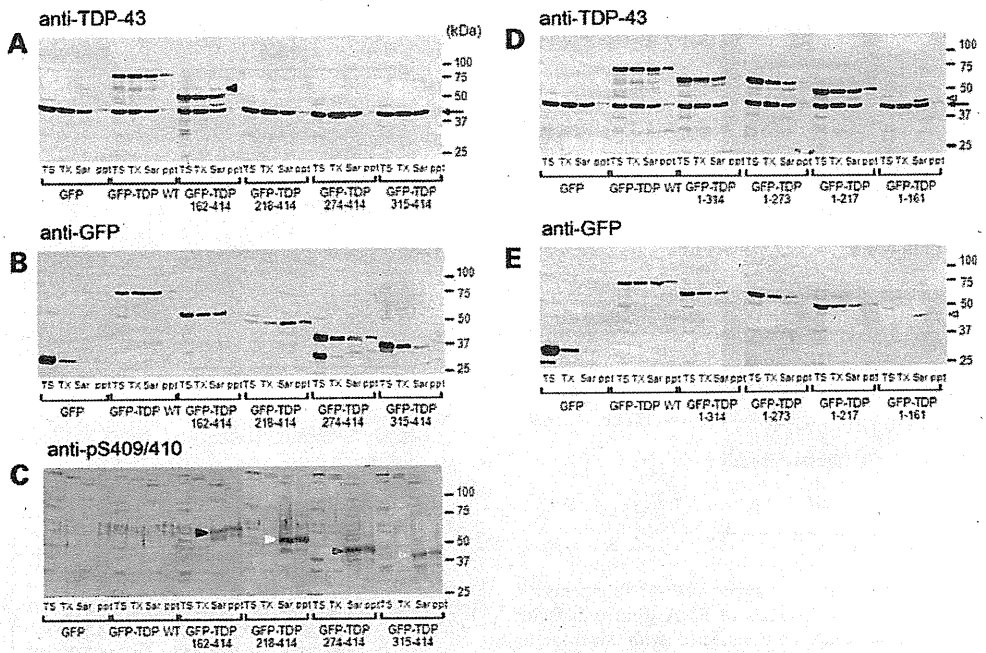

Figure 4. Immunoblot analyses of inclusions composed of GFP-tagged N-terminal and C-terminal fragments of TDP-43. SH-SY5Y cells, 72 h post-transfection with GFP alone or GFP-fused TDP-43 fragments, were sequentially extracted with Tris-saline (TS), 1% Triton X-100 (TX) and 1% Sarkosyl (Sar), and the supernatants and the Sarkosyl-insoluble pellets (ppt) were subjected to SDS–PAGE. Bands were transferred to PVDF membrane and probed with anti-TDP-43 antibody (**A** and **D**), anti-GFP antibody (**B** and **E**) and anti-pS409/410 antibody (**C**). The arrow indicated the band of endogenous TDP-43. Note that bands of pS409/410-positive C-terminal fragments were detected in Sarkosyl-soluble or -insoluble fractions of cells expressing GFP-TDP 162–414 (black arrowhead in C), GFP-TDP 218–414 (white arrowhead in C), GFP-TDP 274–414 (black-lined arrowhead in C) and GFP-TDP 315–414 (white-lined arrowhead in C), and that N-terminal fragment of GFP-TDP 1–161 was recovered in TX-insoluble fractions (black-lined arrowhead in D and E).

the entire RRM-1 motif do not have exon skipping activity, while the wild-type and fragments with the RRM-1 motif have the activity (Figs 1 and 5). These results are in good agreement with the observation by Buratti and Baralle (21) that the RRM-1 domain is necessary for binding with RNA. It is noteworthy that all the TDP-43 fragments which form intracellular aggregates lack exon skipping activity.

Expression of TDP-43 C-terminal fragment facilitates aggregation of full-length TDP-43 in SH-SY5Y cells

To test whether C-terminal fragments of TDP-43 interact with full-length TDP-43, C-terminal fragments of GFP-TDP-43 or full-length GFP-TDP-43 was co-expressed with full-length DsRed-fused TDP-43 (DsRed-TDP-43) in SH-SY5Y cells. Immunoprecipitation experiments of cell lysates using agarose conjugated anti-GFP followed by immunoblotting with anti-RFP or anti-TDP-43 showed that GFP-TDP-43 C-terminal fragments as well as full-length GFP-TDP-43 were bound to full-length DsRed-TDP-43 (Fig. 6). Full-length GFP-TDP-43 was found to more strongly interact with DsRed-TDP-43 than any other C-terminal fragments of GFP-TDP-43. The experiments also showed a weak but notable interaction between endogenous TDP-43 and full-length GFP-TDP-43 or C-terminal fragments of GFP-TDP-43. These results suggest that both full-length GFP-TDP-43 and its C-terminal fragments interact not only with full-length DsRed-TDP-43 but also with endogenous TDP-43 in SH-SY5Y cells.

To monitor the intracellular interaction between endogenous TDP-43 and C-terminal fragments of GFP-TDP-43, SH-SY5Y cells were transfected with GFP-TDP 162–414 or GFP-TDP 218–414 and analyzed by confocal microscopy. Immunostaining using anti-TDP-43 showed that full-length GFP-TDP-43 was co-localized with endogenous TDP-43 in nuclei (Fig. 7A). We observed that GFP signals from cytoplasmic inclusions of GFP-TDP 162–414 or GFP-TDP 218–414 were overlapped with immunoreactivities of anti-TDP-43. Furthermore, immunoreactivities of anti-TDP-43 were almost eliminated from the nuclei of these cells (Fig. 7B and C). When full-length GFP-TDP-43 was co-expressed with full-length DsRed-TDP-43, both proteins were found to be localized in nuclei with no formation of inclusion-like structures (Fig. 7D). In contrast, round cytoplasmic inclusions with both GFP and DsRed signals appeared when GFP-TDP 162–414 (Fig. 7E) or GFP-TDP 218–414 (Fig. 7F) was co-expressed with full-length DsRed-TDP-43. These results indicate that endogenous TDP-43 or exogenous full-length DsRed-TDP-43 is trapped into cytoplasmic inclusions formed by GFP-TDP 162–414 or GFP-TDP 218–414, which is consistent with the results of immunoprecipitation experiments shown in Fig. 6.

Effects of pathogenic mutations on aggregation of TDP-43

Then, we tested the effect of mutations of the TDP-43 gene found in familial and sporadic ALS cases on the intracellular aggregates of C-terminal fragments of GFP-TDP-43 (GFP-TDP 162–414). GFP-TDP 162–414 with or without mutations was expressed in SH-SY5Y cells, which were then analyzed by immunoblot and confocal microscopy. We first confirmed almost same expression levels of all exogenous

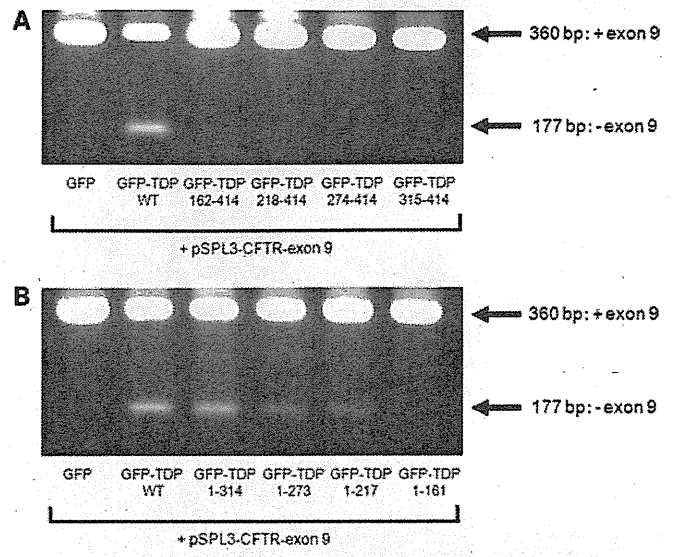

Figure 5. CFTR exon 9 skipping assay of GFP-tagged TDP-43 fragments. (**A** and **B**) Gel electrophoresis of RT–PCR products of RNA from transfected cos-7 cells. The RNAs from cos-7 cells, co-transfected with the reporter plasmid pSPL3-CFTR exon 9 (TG11T7) plus pEGFP-TDP-43 expression vectors, were used as templates for RT–PCR analysis. The products were analyzed by electrophoresis in 1.5% agarose gel.

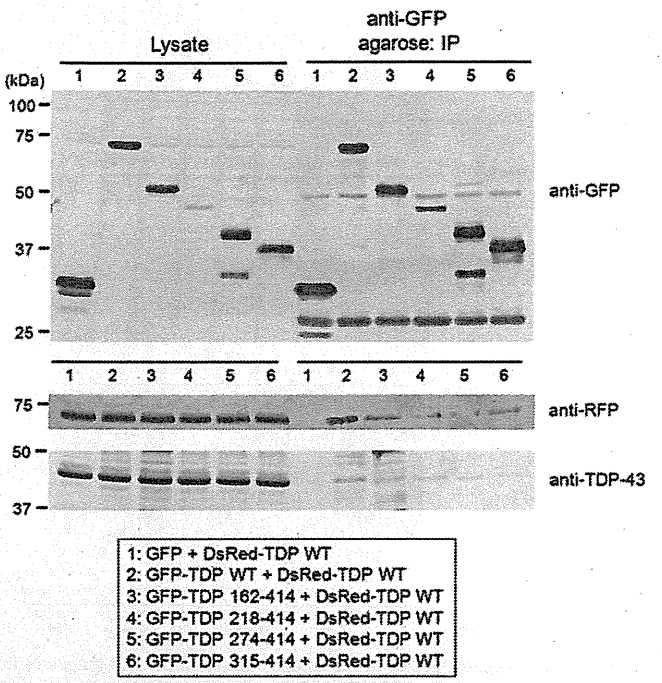

Figure 6. Full-length GFP-TDP-43 and its C-terminal fragments interact not only with full-length DsRed-TDP-43 but also with endogenous TDP-43. SH-SY5Y cells were transfected with pDsRed-TDP-43 wild-type (DsRed-TDP WT) and pEGFP-C1 (GFP; lane 1), pEGFP-TDP-43 WT (GFP-TDP WT; lane 2), pEGFP-TDP 162–414 (GFP-TDP 162–414; lane 3), pEGFP-TDP 218–414 (GFP-TDP 218–414; lane 4), pEGFP-TDP 274–414 (GFP-TDP 274–414; lane 5) or pEGFP-TDP 315–414 (GFP-TDP 315–414; lane 6), for 3 days, and analyzed by immunoprecipitation. Cell lysates (total protein: ~100 μg) was recovered and subjected to IP with agarose conjugated anti-GFP (~5 μg of anti-GFP, MBL). Bounds proteins were eluted from the beads with SDS sample buffer. Each sample (~5 μg of lysates and ~1/5 aliquots of IP fraction) was separated by 10% SDS–PAGE and immunoblotted with anti-GFP antibody, anti-RFP antibody and anti-TDP-43 antibody.

GFP-TDP 162–414 with or without mutations by immunoblot analysis with anti-TDP-43 (Fig. S2). Figure 8 showed that all 14 mutant GFP-TDP 162–414 formed more intracellular aggregates than wild-type GFP-TDP 162–414. Of these mutations, the number of cells with aggregates was significantly higher in GFP-TDP 162–414 with D169G, G294A, Q331K, M337V, Q343R, N390D and N390S, when compared with the wild-type GFP-TDP 162–414 (Fig. 8B).

When full-length TDP-43 with or without GFP fusion was expressed in cells, we could not find any significant difference in the number of cells with aggregates between wild-type and all mutants (data not shown). Furthermore, there was no significant difference in the generation of TDP-43 fragments (Supplementary Material, Fig. S3) or exon skipping activity of CFTR exon 9 between wild-type full-length TDP-43 and mutated full-length TDP-43 (data not shown).

Identification of the cleavage sites of N-terminally truncated TDP-43 fragments in FTLD-U brains

To identify the cleavage sites of the C-terminal fragments of TDP-43 accumulated in brains of FTLD-U patients, we performed protein chemical analyses of the major fragments of 18–26 kDa in the Sarkosyl-insoluble fraction (Fig. 9A). Mass spectra analysis of tryptic digests of these fragments identified two typical tryptic peptides, (K)GISVHISNAEPKHNSNR (residues 252–268) and (R)FGGNPGGFG NQGGFGNSR (residues 276–293), and two unusual tryptic peptides, (M)DVFIPKPFR (residues 219–227) (Fig. 9B) and (E)DLIIK (residues 247–251) (Fig. 9C). N-termini of the latter two peptides are not produced by trypsin, because this enzyme cannot cleave Met218-Asp219 and Glu246-Asp247 bonds. These results suggest that these peptides are N-terminal parts of C-terminal fragments of TDP-43, and that the major C-terminal fragments deposited in FTLD-U brains are produced by cleavage between Met218-Asp219 or Glu246-Asp247.

To characterize these C-terminal fragments of TDP-43 deposited in FTLD-U brains with regards to intracellular aggregates formation, phosphorylation, and CFTR exon 9 splicing activity, GFP-TDP 219–414 and GFP-TDP 247–414 were constructed and expressed in SH-SY5Y cells for 3 days. These cells were analyzed using confocal microscopy, immunoblot and CFTR exon 9 skipping assay. As shown in Fig. 10A, round cytoplasmic inclusions with GFP fluorescence were clearly observed in cells expressing GFP-TDP 219–414 or GFP-TDP 247–414. These were also positive for anti-pS409/410 and anti-Ub. In immunoblot analyses, GFP-TDP 219–414 and GFP-TDP 247–414 were detected in Sar-soluble and insoluble fractions with anti-pS409/410 (Fig. 10B). These results suggest that these C-terminal fragments have high propensity to aggregate in cells, which is in good agreement with above results obtained from cells expressing other C-terminal fragments (e.g. GFP-TDP 218–414). Furthermore, expression of each C-terminal fragment resulted in a decrease in exon 9 skipping activity relative to GFP-TDP wild-type, as shown in Fig. 10C. We also found that overexpression of these C-terminal fragments led to a slight but

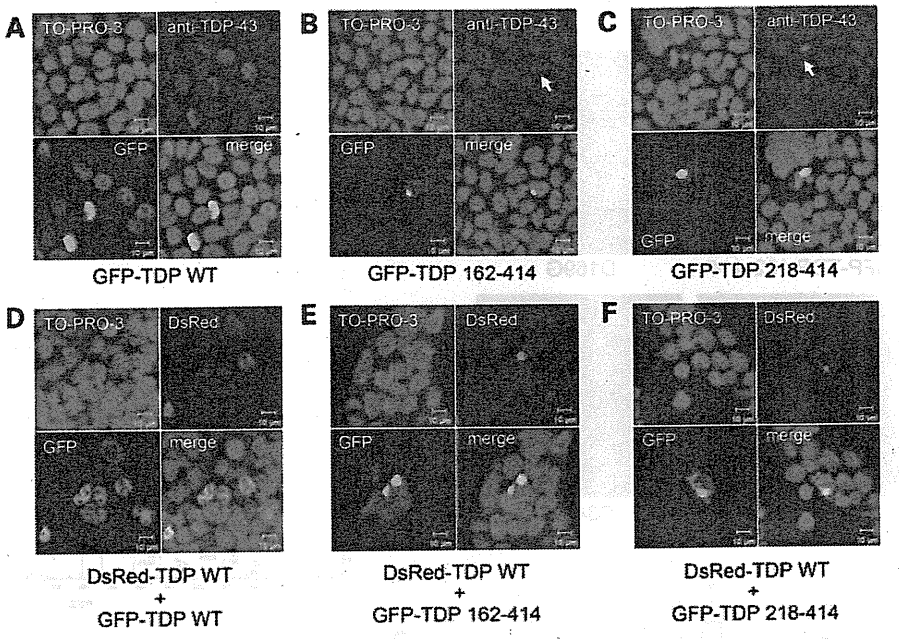

Figure 7. Co-expression of both DsRed-TDP-43 wild-type and GFP-TDP-43 wild-type or its C-terminal fragments. SH-SY5Y cells were transfected with pEGFP-TDP-43 wild-type (GFP-TDP WT), pEGFP-TDP 162–414 (GFP-TDP 162–414), pEGFP-TDP 218–414 (GFP-TDP 218–414) with (**D**–**F**) or without pDsRed-TDP-43 WT (**A**–**C**) for 3 days, and analyzed by confocal microscopy. Endogenous TDP-43 was stained by anti-TDP-43 antibody (ProteinTech) in (A–C). DNA was stained with TO-PRO-3. The threshold gain level of laser power (543 nm for detection of DsRed) was adjusted so that the signals did not overlap. Immunoreactivities of anti-TDP-43 were almost eliminated from the nuclei of cells with inclusions of GFP-TDP 162–414 (arrow in B) and GFP-TDP 218–414 (arrow in C).

significant increase in CFTR exon 9 inclusion (Fig. 10C, lower panel). This result suggests that endogenous TDP-43 was trapped with these aberrant C-terminal fragments, resulting a loss of exon 9 exclusion activity by endogenous TDP-43.

DISCUSSION

In this work, we showed that expression of C-terminal and N-terminal fragments of TDP-43 as GFP fusions resulted in the formation of phosphorylated and ubiquitinated aggregates in cultured cells. We first tried to express non-tagged C-terminal TDP-43 fragment (residues 162–414 or 218–414) in SH-SY5Y cells, but without success (data not shown). We then constructed plasmids encoding GFP-tagged N-terminal and C-terminal fragments of TDP-43, as shown in Fig. 1. The C-terminal fragments were significantly more prone to aggregate than full-length TDP-43. These aggregated C-terminal fragments were phosphorylated at Ser409 and Ser410, and were recovered in the TX-insoluble and Sar-soluble as well as Sar-insoluble fractions. These features are consistent with our previous findings, which showed that phosphorylated C-terminal fragments of TDP-43 were the major component of Sar-insoluble TDP-43 in the FTLD-U and ALS brains (15).

Recently, Johnson *et al.* (22) reported a yeast TDP-43 proteinopathy model. They found that RRM-2 and a C-terminal region (188–414 residues) are required for TDP-43 to form toxic aggregates. The fact that the highest propensity to aggregate was seen with GFP-TDP 162–414 and GFP-TDP 218–414 in the present study is consistent with their observations. However, the formation of pS409/410-positive inclusion-like structures in cells expressing C-terminal fragments without RRM2 (GFP-TDP 274–414 and 315–414), and the lack of striking cell death in cells expressing any GFP-tagged TDP-43 fragments (data not shown), differ from their findings. Furthermore, we could not detect intracellular aggregates formed by full-length GFP-TDP-43 in this study. One of the reasons for such discrepancies may be the differences between cultured neuronal cells and yeast.

We also found that one of the N-terminal fragments of TDP-43, GFP-TDP 1-161 were also prone to aggregate in cultured cells. This fragment was recovered in the TX-insoluble and Sar-soluble fraction. Previous reports indicated that lower-molecular-weight bands were present in the Sar-insoluble fractions of FTLD-U cases using the anti-TDP-43 (ProteinTech) (2,3,23). In this study, we established that this antibody recognizes the epitopes in the N-terminal portion between the residues 1 and 217 but not the C-terminal portion. Therefore, N-terminal fragments of TDP-43 may be present in the Sar-insoluble fraction of FTLD-U samples. It is noteworthy, therefore, that the expression of N-terminal TDP-43 fragments, as well as C-terminal fragments, could cause the formation of cytoplasmic aggregates in cultured cells.

The results of co-expression experiments using GFP-TDP 162–414 or GFP-TDP 218–414 and full-length DsRed-TDP-43 (Fig. 7) are consistent with the notion that cytoplasmic aggregates of C-terminal fragments of TDP-43 initially formed recruit newly synthesized full-length TDP-43 monomer and stay it in cytoplasm, resulting in depleting normal nuclear TDP-43. This may explain why normal TDP-43 staining is cleared in nuclei of diseased neurons containing cytoplasmic TDP-43 aggregates. Such mislocalization of full-length TDP-43 may induce neuronal dysfunction due to loss of

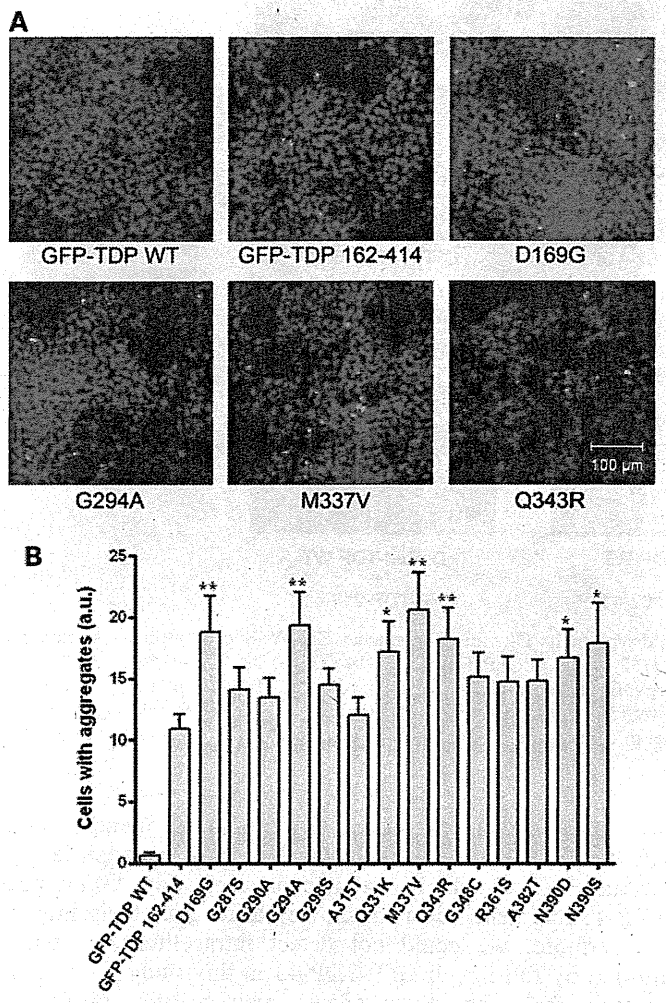

Figure 8. The effects of pathogenic mutations found in familial and sporadic ALS on intracellular accumulations of GFP-tagged TDP-43 C-terminal fragment. SH-SY5Y cells were transfected with GFP-TDP-43 wild-type (GFP-TDP WT), GFP-TDP 162-414 or each of 14 mutants (D169G, G287S, G290A, G294A, G298S, A315T, Q331K, M337V, Q343R, G348C, R361S, A382T, N390D and N390S) for 3 days, fixed and analyzed by confocal microscopy. DNA was stained with TO-PRO-3. (**A**) Images from cells transfected with GFP-TDP WT, GFP-TDP 162–414, GFP-TDP 162–414 with D169G (D169G), G294A (G294A), M337V (M337V) and Q343R (Q343R) were shown. (**B**) The rates of cells including intracellular aggregates were calculated in arbitrary units. Fluorescence intensity within an area of ~800 × 800 μm was assessed by confocal microscopy. The intensity of GFP was calculated as a ratio to that of TO-PRO-3. More than eight areas per sample were measured ($n = 8–16$). Data are means ± SEM. $^{*}P < 0.05$; $^{**}P < 0.01$ by Student's *t*-test against the value of GFP-TDP 162–414.

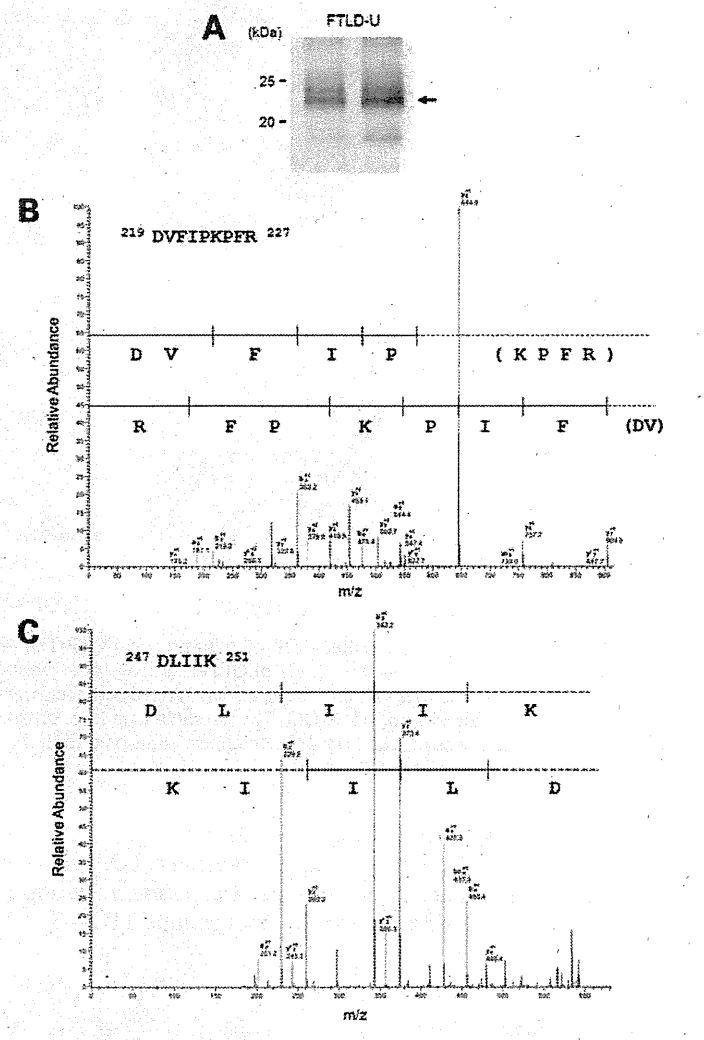

Figure 9. Identification of the cleavage site of TDP-43 C-terminal fragments deposited in FTLD-U brains. (**A**) C-terminal fragments of TDP-43 deposited in FTLD-U brains were detected with anti-pS409/410 (15). The pS409/410-positive ~23 kDa bands (an arrow) were dissected and digested in-gel with trypsin. (**B** and **C**) Product ion spectra of a mass signal $(M+2H)^{2+}$ of m/z 560.55 (B) and m/z 601.71 (C) from tryptic digests of urea-soluble C-terminal fragment of TDP-43 from FTLD-U brains. These spectra show the b and y ion series, identifying the peptide, DVFIPKPFR (residues 219–227) and DLIIK (residues 247–251), respectively. Vertical bars denote consecutive mass signals in b and y series.

physiological functions of TDP-43 in nuclei (3,17). In this study, we showed that expression of aberrant C-terminal fragment (GFP-TDP 219–414 or 247–414) resulted in decreased activity of CFTR exon 9 exclusion by endogenous TDP-43 due to its mislocalization in cytoplasm. It is also noteworthy that exogenously expressed full-length TDP-43 binds to each other, and the interaction between full-length TDP-43 is stronger than that between C-terminal fragments and full-length TDP-43. These results suggest that N-terminal portion may be essential for an inter-TDP-43 binding, which may contribute to its structural stability.

Interestingly, all TDP-43 fragments which form cytoplasmic aggregates lack CFTR exon 9 skipping activity (Figs 1 and 5). It was reported that the entire RRM-1 domain and C-terminal glycine-rich domain are required for CFTR exon 9 skipping (21,24–26). TDP-43 is considered to bind to hnRNP A/B through this domain (24). In our hands, all C-terminal fragments in this study lack skipping activity of CFTR exon 9, although these fragments retain the glycin-rich domain. Absence of RRM-1 or formation of cytoplasmic aggregates or both might impair the physiological functions of TDP-43, leading to cellular dysfunction and neurodegeneration. Further studies are needed to examine whether or not cellular function(s) (proliferation, differentiation, etc.) are affected in cells expressing TDP-43 fragments without the RRM-1 or glycine-rich domain or both.

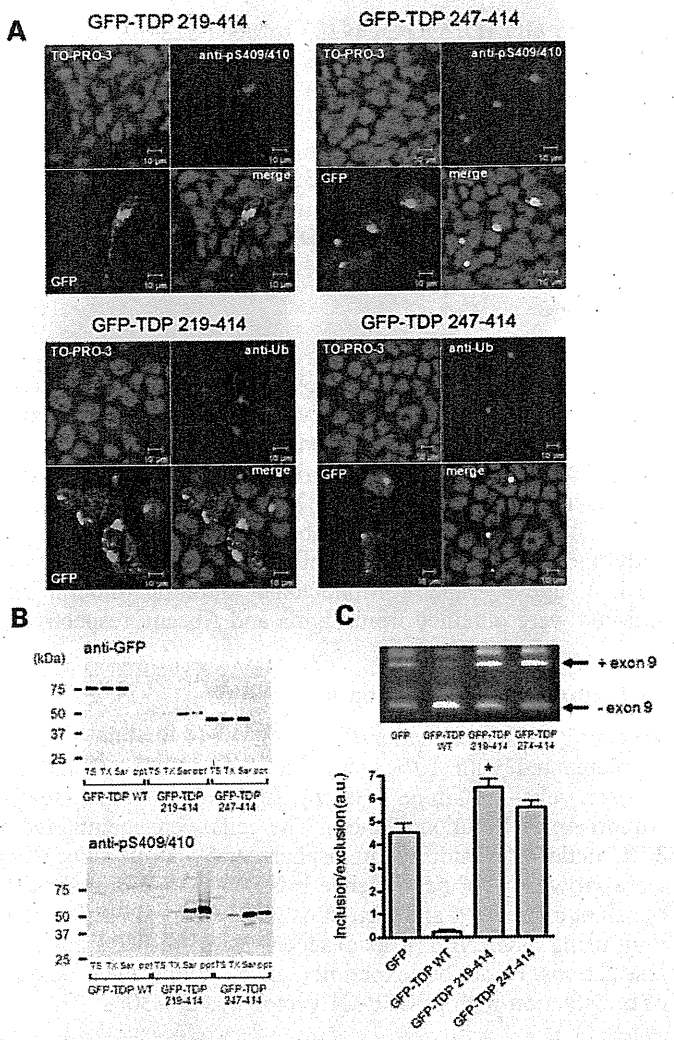

Figure 10. Pathological characterization of C-terminal fragments of TDP-43 identified in FTLD-U brains. (**A**) Confocal microscopic analyses of cells expressing GFP-TDP 219–414 (left) and GFP-TDP 247–414 (right). SH-SY5Y cells 72 h post-transfection with GFP-TDP 219–414 and GFP-TDP 247–414 were stained with anti-pS409/410 (upper) and anti-Ub (lower). (**B**) Immunoblot analyses of cells expressing GFP-TDP 219–414 and GFP-TDP 247–414. SH-SY5Y cells, 72 h post-transfection, were sequentially extracted with Tris-saline (TS), 1% Triton X-100 (TX) and 1% Sarkosyl (Sar), and the supernatants and the Sarkosyl-insoluble pellets (ppt) were subjected to SDS–PAGE. Bands were transferred to PVDF membrane and probed with anti-GFP antibody and anti-pS409/410 antibody. (**C**) CFTR exon 9 splicing assay. Gel electrophoresis of RT–PCR products of RNA from transfected cos-7 cells. The RNAs from cos-7 cells, co-transfected with the reporter plasmid pSPL3-CFTR exon 9 (TG13T5) plus pEGFP-TDP-43 expression vectors, were used as templates for RT–PCR analysis. The products were analyzed by electrophoresis in 1.5% agarose gel. The lower panel shows quantitative analyses of the ratio of CFTR exon 9 inclusion/exclusion. The intensity of each band was analysed using the Image J software. Data ($n = 4$) are means ± SEM. $^*P < 0.05$ by Student's *t*-test against the value of GFP.

Several groups have recently reported increased accumulation of TDP-43 fragments in the brain homogenates (8) and cultured cells (5,6) in some of the pathogenic mutations in ALS. The major component of abnormally accumulated TDP-43 is the C-terminal fragments in all TDP-43 proteinopathy (15,23). In this study, however, immunoblot analyses using a commercial TDP-43 antibody and our C-terminal 405–414 antibody (15,19) failed to show any significant differences in the generation of fragments of TDP-43 with or without various mutations (Supplementary Material, Fig. S3). The results of this study provide evidence, for the first time, that all 14 mutations tested consistently enhance aggregation of TDP-43 if they are present in the C-terminal fragments. We examined the effects of TDP-43 mutations on aggregates formation of both GFP-TDP 162–414 and GFP-TDP 218–414. We found that mutations significantly facilitate the formation of cytoplasmic inclusions of GFP-TDP 162–414, but not GFP-TDP 218–414 (data not shown). In this study, GFP-TDP 218–414 was found to be most prone to aggregate in SH-SY5Y cells. Thus, it seems likely that the high propensity to aggregate formation of GFP-TDP 218–414 may mask mutation effects on aggregates formation of GFP-TDP 218–414. So, we speculate that mutation effects were significantly detected in the experiments using GFP-TDP 162–414 which was less prone to form cytoplasmic inclusions than GFP-TDP 218–414. It seems reasonable to speculate that pathogenic mutations and N-terminal truncation synergistically promote abnormal accumulation of TDP-43. Failure to form aggregates in cells that express mutated full length TDP-43 suggests that the cell culture models recapitulate *in vivo* diseases only partially and that such models need N-terminal truncation of TDP-43 as a prerequisite for the mutation effect.

Igaz *et al.* (27) reported the cleavage site at Arg 208 in a pathological TDP-43 C-terminal fragment from FTLD-U brains and inclusion formation in cultured cells expressing resultant C-terminal fragment (residues 208–414). In the present study, by mass spectrometric analysis of the sarkosyl-insoluble fraction extracted from the FTLD-U brains, we newly identified two C-terminal fragments generated by N-terminal truncation at Asp219 and Asp247 of TDP-43 (196 and 168 amino acids, respectively). It should be noted that of these, the fragment cleaved at Asp219 (residues 219–414) is almost identical to TDP 218–414 employed in this study, which we found to be the most prone to aggregate in SH-SY5Y cells. We also confirmed that phosphorylated and ubiquitinated cytoplasmic inclusions were formed in cells expressing GFP-TDP 219–414 or GFP-TDP 247–414. Thus, the generation of aggregation-prone fragments of TDP-43 may play an important role for pathological process of TDP-43 proteinopathy. The N-termini of both identified peptides were Asp residue, suggesting that the protease(s) responsible for the cleavage may show specificity for the N-terminal side of Asp residues. Regarding the protease to degrade TDP-43, Zhang *et al.* (28) previously reported the occurrence of caspase cleavage of TDP-43 in cultured cells by the knockdown of progranulin gene. Furthermore, they recently reported the formation of intracellular inclusions immunopositive for phosphorylated TDP-43 and ubiquitin in cells expressing the GFP-tagged C-terminal fragment of TDP-43 (residues 220–414), which is expected to be generated by caspase cleavage (29). In the present study, however, we did not detect VFIPKPFR (residues 220–227), which is predicted to be produced by trypsin digestion of caspase-cleaved TDP-43, in the sarkosyl-insoluble fraction from the FTLD-U brains. These results suggest that caspase may not be the responsible enzyme for generation of

C-terminal fragments of TDP-43 in human brains. Since several abnormal fragments of 18–26 kDa were detected in FTLD-U and ALS with the antibodies to C-terminal region of TDP-43 like anti-pS409/410 (15, 19, 23), it seems reasonable to speculate the presence of the multiple cleavage sites in the middle of TDP-43. Thus, there may be other fragments, the N-termini of which have yet to be identified, and its responsible proteases. Further investigation of the degradation mechanism of TDP-43 might be needed to elucidate the pathogenesis of TDP-43 proteinopathy.

Our findings here provide further support for the idea that accumulation of fragmented TDP-43 plays an important role in TDP-43 proteinopathy. Our cellular models are expected to be useful tools to investigate the pathogenesis of TDP-43 proteinopathy, since they show pathological and biochemical characteristics similar to those of inclusions found in brains of patients, in terms of size, abnormal phosphorylation and ubiquitination.

MATERIALS AND METHODS

Construction of plasmids

To construct N-terminally green fluorescent protein (GFP)- and DsRed-fused TDP-43, a cDNA encoding full-length TDP-43 was amplified from pcDNA3-TDP-43 using the following primers: GFP/DsRed-forward, 5′-CCGCTCGAGCTA TGTCTGAATATATTCGGGTAACCGAA-3′; GFP/DsRed-reverse, 5′-CGGGATCCCTACATTCCCCAGCCAGAAG-3′. The amplified fragment was digested with *Xho*I/*Bam*HI and was cloned into the same cleavage sites of the pEGFP-C1 vector (Clontech) and pDsRed-Monomer-C1 vector (Clontech), respectively. For the construction of GFP-tagged TDP-43 fragments, each fragment was amplified by PCR using the following primers: for GFP-tagged TDP-43 fragment of residues 162–414 (GFP-TDP 162–414), forward, 5′-CC GCTCGAGCTATGTCACAGCGACATATGA-3′ and GFP/DsRed-reverse; for GFP-TDP 218–414, forward, 5′-CCGCT CGAGCTATGGATGTCTTCATCCCCA-3′ and GFP/DsRed-reverse; for GFP-TDP 219–414, forward, 5′-CCGCTCGAGCT GATGTCTTCATCCCCAAGCC-3′ and GFP/DsRed-reverse; for GFP-TDP 247–414, forward, 5′-CCGCTCGAGCT GACTTGATCATTAAAGGAAT-3′ and GFP/DsRed-reverse; for GFP-TDP 274–414, forward, 5′-CCGCTCGAGCTGGAAGATTTGGTGGTAATCCA-3′ and GFP/DsRed-reverse; for GFP-TDP 315–414, forward, 5′-CCGCTCGAGCTGCGTTCAGCATTAATCCAGCCAT-3′ and GFP/DsRed-reverse; for GFP-TDP 1–161, GFP/DsRed-forward and reverse, 5′-CGGGATCCCTATACTTTCACTT GTGTTT-3′; for GFP-TDP 1–217, GFP/DsRed-forward and reverse, 5′-CGGGATCCCTACACATCCCCGTACTGAG-3′; for GFP-TDP 1–273, GFP/DsRed-forward and reverse, 5′-CGGGATCCCTAACTTCTTTCTAACTGTCTATTGCT-3′; for GFP-TDP 1–314, GFP/DsRed-forward and reverse, 5′-CG GGATCCCTAACCAAAGTTCATCCCACCACCCAT-3′. The resulting products were digested with *Xho*I/*Bam*HI and were cloned into the same cleavage sites of the pEGFP-C1 vector (Clontech). Site-directed mutagenesis of GFP-tagged or non-tagged full-length TDP-43 and GFP-tagged C-terminal fragment (GFP-TDP 162–414) was carried out to substitute Asp169 to Gly (D169G), Gly287 to Ser (G287S), Gly290 to Ala (G290A), Gly294 to Ala (G294A), Gly298 to Ser (G298S), Ala315 to Thr (A315T), Gln331 to Lys (Q331K), Met337 to Val (M337V), Gln343 to Arg (Q343R), Gly348 to Cys (G348C), Arg361 to Ser (R361S), Ala382 to Thr (A382T), Asn390 to Asp (N390D) and Asn390 to Ser (N390S) using a site-directed mutagenesis kit (Strategene). All constructs were verified by DNA sequencing.

Antibodies

A polyclonal TDP-43 antibody 10782-1-AP (anti-TDP-43) was purchased from ProteinTech Group Inc. A polyclonal antibody specific for phosphorylated TDP-43 (anti-pS409/410) and anti-405-414 antibody specific for C-terminal TDP-43 were prepared as described (15,19). Anti-ubiquitin monoclonal antibody (mAb), MAB1510, was purchased from Chemicon. Anti-GFP mAb, anti-RFP polyclonal antibody and agarose-conjugated anti-GFP were purchased from MBL (Nagoya, Japan). Monoclonal anti-alpha-tubulin and anti-p84 were obtained from Sigma and Abcam, respectively.

Cell culture and expression of plasmids

SH-SY5Y cells were cultured in DMEM/F12 medium (Sigma) supplemented with 10% (v/v) fetal calf serum, penicillin–streptomycin–glutamine (Gibco), and MEM Non-Essential Amino Acids Solution (Gibco). The cells were maintained at 37°C under a humidified atmosphere of 5% (v/v) CO_2. They were grown to 50% confluence in six-well culture dishes for transient expression and then transfected with expression plasmids using FuGENE6 (Roche) according to the manufacturer's instructions. Under our experimental conditions, the efficiency of transfection with pEGFP-C1 vector was 20–30%.

Confocal immunofluorescence microscopy

SH-SY5Y cells were grown on a coverslip (15 × 15 mm) and transfected with expression vector(s) (1 or 2 μg). After incubation for the indicated time, the transfected cells on the coverslips were fixed with 4% (w/v) paraformaldehyde in phosphate-buffered saline (PBS) for 30 min. The coverslips were then incubated in 50 mM NH_4Cl in PBS for 10 min and cell permeabilization was performed with 0.2% (v/v) Triton X-100 in PBS for 10 min. After blocking for 30 min in 5% (w/v) BSA in PBS, cells were incubated with anti-phosphorylated TDP-43 antibody, anti-pS409/410 (1:500 dilution) and anti-Ub (1:500) for 1 h at 37°C, followed by Alexa Fluor 488- or Alexa Fluor 568-labeled goat anti-rabbit or-mouse IgG (Invitrogen, 1:1000 dilution) for 1 h at 37°C. After washing, the cells were further incubated with TO-PRO-3 (Invitrogen, 1:3000 dilution in PBS) for 1 h at 37°C to stain nuclear DNA, and analyzed using an LSM5 Pascal confocal laser microscope (Carl Zeiss).

Intracellular aggregates of GFP-tagged TDP-43 fragments had much more intense fluorescence of GFP than diffusely expressed, GFP-tagged wild-type TDP-43 or GFP alone. Therefore, to quantify the cells with GFP-tagged TDP-43 aggregates, the laser power (at 488 nm for detection of GFP) was adjusted so that only the aggregates were detected (30).

Total intensity of GFP fluorescence detected at the threshold laser power and that of TO-PRO-3 fluorescence, the latter corresponding to the total number of cells, in a given field (~800 × 800 μm) were measured with LSM5 Pascal v 4.0 software (Carl Zeiss) and the ratios of cells with inclusions were calculated.

In the co-expression experiments with combinations of GFP-tagged TDP 162–414 or TDP 218–414 and DsRed-tagged wild-type TDP-43, the laser power (at 543 nm for detection of DsRed) was appropriately adjusted so that the signals did not overlap.

Sequential extraction of proteins and immunoblotting

SH-SY5Y cells were grown in six-well plates and transfected transiently with expression plasmids (1 μg). After incubation for the indicated time, cells were harvested and lysed in TS buffer [50 mM Tris–HCl buffer, pH 7.5, 0.15 M NaCl, 5 mM ethylenediaminetetraacetic acid (EDTA), 5 mM ethylene glycol bis (β-aminoethyl ether)-*N,N,N,N*-tetraacetic acid (EGTA) and protease inhibitor cocktail (Roche)]. The lysates were centrifuged at 290 000*g* for 20 min at 4°C, and the supernatant was recovered as the TS-soluble fraction. The TS-insoluble pellets were lysed in TS buffer containing 1% (v/v) Triton X-100 (TX) and centrifuged at 290 000*g* for 20 min at 4°C. The supernatant was collected as the TX-soluble fraction. The TX-insoluble pellets were further sonicated in TS buffer containing 1% (w/v) Sarkosyl (Sar) and incubated for 30 min at 37°C. The mixtures were centrifuged at 290 000*g* for 20 min at room temperature and the supernatant was recovered as the Sar-soluble fraction. The remaining pellets (insoluble in Sar) were lysed in SDS-sample buffer and heated for 5 min.

Subcellular fractionation was performed using NE-PER nuclear and cytoplasmic extraction reagents (Pierce) according to the manufacturer's instructions. SH-SY5Y cells were grown in six-well plates and transfected transiently with expression plasmids (1 μg). After incubation for 48 h, cells were harvested and fractionated into nuclear and cytoplasmic fraction using NE-PER.

Protein concentration was estimated using the BCA Protein Assay Kit (Pierce). Each sample (10 or 20 μg) was separated by 10 or 12% (v/v) SDS–PAGE using Tris–glycine buffer system, and proteins were transferred onto polyvinylidene difluoride membrane (Millipore). The blots were blocked with 3% (v/v) gelatin and incubated overnight with the indicated primary antibody in 10% (v/v) calf serum at an appropriate dilution (1:1000–5000) at room temperature. The membranes were washed and then incubated with a biotin-labeled secondary antibody (Vector) for 2 h or a horse radish peroxidase-labeled secondary antibody (BIO-RAD) for 1 h at room temperature. Signals were detected using the ABC staining kit (Vector) or ECL Plus Western Blotting Detection System (GE Healthcare).

CFTR exon 9 skipping assay

Cos-7 cells grown in six-well plates were transfected with 0.5 μg of the reporter plasmid pSPL3-CFTR9 (including a TG11T7 (16) or TG13T5 sequence) plus 1 μg of pEGFP plasmid encoding wild-type TDP-43 or its fragment, using FuGENE6. The cells were harvested 48 h post-transfection and total RNA was extracted with TRIzol (Invitrogen). The cDNA was synthesized from 1 μg of total RNA with the use of the Superscript II system (Invitrogen). Primary and secondary PCRs were carried out according to the instruction manual of the exon trapping system (Life Technologies).

Immunoprecipitation

SH-SY5Y cells grown in six-well plates were transfected with expression vectors (total 2 μg). After incubation for 3 days, cells were harvested and lysed in RIPA buffer [50 mM Tris–HCl buffer, pH 7.5, 0.15 M NaCl, 1% NP-40, 0.5% deoxycholic acid Na, 0.1% SDS, 5 mM EDTA, 5 mM EGTA, 1 mM PMSF and protease inhibitor cocktail (Roche)]. The lysates were centrifuged at 20 400*g* for 10 min at 4°C and the supernatant (total protein: ~100 μg) was recovered and subjected to IP with agarose conjugated anti-GFP [20 μl of 50% gel slurry (~5 μg of anti-GFP), MBL]. Bound proteins were washed with RIPA buffer and then eluted from the beads with SDS sample buffer. Each sample was separated by 10% SDS–PAGE and immunoblotted with anti-GFP mAb (MBL), anti-RFP polyclonal antibody (MBL) and anti-TDP-43 (ProteinTech).

Mass spectrometric analysis of C-terminal fragments of TDP-43

Sarkosyl-insoluble, 8 M urea soluble fractions prepared from the brain of patients with FTLD-U were subjected to reversed phase-HPLC on an Aquapore RP-300 column (4.6 × 30 mm, Brownlee columns) and fractionated samples were immunoblotted with anti-pS409/410. The positive fraction was lyophilized, treated with SDS-sample buffer and loaded on 15% SDS–PAGE. The pS409/410-positive ~23 kDa bands (Fig. 9A) were dissected and digested in-gel with trypsin. The digests were applied to the Paradigm MS4 HPLC system (Microm BioResources). A reversed phase capillary column (Develosil ODS-HG5, 0.075 × 150 mm, Nomura Chemical) was used at a flow rate of 300 nm/min with a 4–80% linear gradient of acetonitrile in 0.1% formic acid. Eluted peptides were directly detected with an ion trap mass spectrometer, LXQ (Thermo Electron). The obtained spectra were analyzed with BioWorks (Thermo Electron) and Mascot (Matrix Science).

Statistical analysis

The *P*-values for the description of the statistical significance of differences were calculated by means of the unpaired, two-tailed Student's *t*-test using Prism 4 software.

SUPPLEMENTARY MATERIAL

Supplementary Material is available at *HMG* online.

ACKNOWLEDGEMENTS

We thank Dr H. Mimuro (University of Tokyo) for helpful advice and discussions.

Conflict of Interest statement. None declared.

FUNDING

This work was supported by a Grant-in-Aid for Scientific Research on Priority Areas–Research on Pathomechanisms of Brain Disorders (to M.H., 20023038), and Grants-in-Aid for Scientific Research to M.H. (18300117) and F.K. (20300144) and to T.N. (19590297) and T.A. (19591024) from the Ministry of Education, Culture, Sports, Science and Technology of Japan.

REFERENCES

1. Snowden, J.S., Neary, D. and Mann, D.M. (2002) Frontotemporal dementia. *Br. J. Psychiatry.*, **180**, 140–143.
2. Arai, T., Hasegawa, M., Akiyama, H., Ikeda, K., Nonaka, T., Mori, H., Mann, D., Tsuchiya, K., Yoshida, M., Hashizume, Y. *et al.* (2006) TDP-43 is a component of ubiquitin-positive tau-negative inclusions in frontotemporal lobar degeneration and amyotrophic lateral sclerosis. *Biochem. Biophys. Res. Commun.*, **351**, 602–611.
3. Neumann, M., Sampathu, D.M., Kwong, L.K., Truax, A.C., Micsenyi, M.C., Chou, T.T., Bruce, J., Schuck, T., Grossman, M., Clark, C.M. *et al.* (2006) Ubiquitinated TDP-43 in frontotemporal lobar degeneration and amyotrophic lateral sclerosis. *Science*, **314**, 130–133.
4. Gitcho, M.A., Baloh, R.H., Chakraverty, S., Mayo, K., Norton, J.B., Levitch, D., Hatanpaa, K.J., White, C.L. III, Bigio, E.H., Caselli, R. *et al.* (2008) TDP-43 A315T mutation in familial motor neuron disease. *Ann. Neurol.*, **63**, 535–538.
5. Kabashi, E., Valdmanis, P.N., Dion, P., Spiegelman, D., McConkey, B.J., Vande Velde, C., Bouchard, J.P., Lacomblez, L., Pochigaeva, K., Salachas, F. *et al.* (2008) TARDBP mutations in individuals with sporadic and familial amyotrophic lateral sclerosis. *Nat. Genet.*, **40**, 572–574.
6. Sreedharan, J., Blair, I.P., Tripathi, V.B., Hu, X., Vance, C., Rogelj, B., Ackerley, S., Durnall, J.C., Williams, K.L., Buratti, E. *et al.* (2008) TDP-43 mutations in familial and sporadic amyotrophic lateral sclerosis. *Science*, **319**, 1668–1672.
7. Van Deerlin, V.M., Leverenz, J.B., Bekris, L.M., Bird, T.D., Yuan, W., Elman, L.B., Clay, D., Wood, E.M., Chen-Plotkin, A.S., Martinez-Lage, M. *et al.* (2008) TARDBP mutations in amyotrophic lateral sclerosis with TDP-43 neuropathology: a genetic and histopathological analysis. *Lancet. Neurol.*, **7**, 409–416.
8. Yokoseki, A., Shiga, A., Tan, C.F., Tagawa, A., Kaneko, H., Koyama, A., Eguchi, H., Tsujino, A., Ikeuchi, T., Kakita, A. *et al.* (2008) TDP-43 mutation in familial amyotrophic lateral sclerosis. *Ann. Neurol.*, **63**, 538–542.
9. Benajiba, L., Le Ber, I., Camuzat, A., Lacoste, M., Thomas-Anterion, C., Couratier, P., Legallic, S., Salachas, F., Hannequin, D., Decousus, M. *et al.* (2009) TARDBP mutations in motoneuron disease with frontotemporal lobar degeneration. *Ann. Neurol.*, **65**, 470–473.
10. Deng, H.X., Hentati, A., Tainer, J.A., Iqbal, Z., Cayabyab, A., Hung, W.Y., Getzoff, E.D., Hu, P., Herzfeldt, B., Roos, R.P. *et al.* (1993) Amyotrophic lateral sclerosis and structural defects in Cu,Zn superoxide dismutase. *Science*, **261**, 1047–1051.
11. Rosen, D.R., Siddique, T., Patterson, D., Figlewicz, D.A., Sapp, P., Hentati, A., Donaldson, D., Goto, J., O'Regan, J.P., Deng, H.X. *et al.* (1993) Mutations in Cu/Zn superoxide dismutase gene are associated with familial amyotrophic lateral sclerosis. *Nature*, **362**, 59–62.
12. Mackenzie, I.R., Bigio, E.H., Ince, P.G., Geser, F., Neumann, M., Cairns, N.J., Kwong, L.K., Forman, M.S., Ravits, J., Stewart, H. *et al.* (2007) Pathological TDP-43 distinguishes sporadic amyotrophic lateral sclerosis from amyotrophic lateral sclerosis with SOD1 mutations. *Ann. Neurol.*, **61**, 427–434.
13. Tan, C.F., Eguchi, H., Tagawa, A., Onodera, O., Iwasaki, T., Tsujino, A., Nishizawa, M., Kakita, A. and Takahashi, H. (2007) TDP-43 immunoreactivity in neuronal inclusions in familial amyotrophic lateral sclerosis with or without SOD1 gene mutation. *Acta. Neuropathol.*, **113**, 535–542.
14. Piao, Y.S., Wakabayashi, K., Kakita, A., Yamada, M., Hayashi, S., Morita, T., Ikuta, F., Oyanagi, K. and Takahashi, H. (2003) Neuropathology with clinical correlations of sporadic amyotrophic lateral sclerosis: 102 autopsy cases examined between 1962 and 2000. *Brain Pathol.*, **13**, 10–22.
15. Hasegawa, M., Arai, T., Nonaka, T., Kametani, F., Yoshida, M., Hashizume, Y., Beach, T.G., Buratti, E., Baralle, F., Morita, M. *et al.* (2008) Phosphorylated TDP-43 in frontotemporal lobar degeneration and amyotrophic lateral sclerosis. *Ann. Neurol.*, **64**, 60–70.
16. Nonaka, T., Arai, T., Buratti, E., Baralle, F.E., Akiyama, H. and Hasegawa, M. (2009) Phosphorylated and ubiquitinated TDP-43 pathological inclusions in ALS and FTLD-U are recapitulated in SH-SY5Y cells. *FEBS Lett.*, **583**, 394–400.
17. Winton, M.J., Igaz, L.M., Wong, M.M., Kwong, L.K., Trojanowski, J.Q. and Lee, V.M. (2008) Disturbance of nuclear and cytoplasmic TAR DNA-binding protein (TDP-43) induces disease-like redistribution, sequestration, and aggregate formation. *J. Biol. Chem.*, **283**, 13302–13309.
18. Ayala, Y.M., Zago, P., D'Ambrogio, A., Xu, Y.F., Petrucelli, L., Buratti, E. and Baralle, F.E. (2008) Structural determinants of the cellular localization and shuttling of TDP-43. *J. Cell Sci.*, **121**, 3778–3785.
19. Inukai, Y., Nonaka, T., Arai, T., Yoshida, M., Hashizume, Y., Beach, T.G., Buratti, E., Baralle, F.E., Akiyama, H., Hisanaga, S.I. *et al.* (2008) Abnormal phosphorylation of Ser409/410 of TDP-43 in FTLD-U and ALS. *FEBS Lett.*, **582**, 2899–2904.
20. Buratti, E., Dork, T., Zuccato, E., Pagani, F., Romano, M. and Baralle, F.E. (2001) Nuclear factor TDP-43 and SR proteins promote *in vitro* and *in vivo* CFTR exon 9 skipping. *EMBO J.*, **20**, 1774–1784.
21. Buratti, E. and Baralle, F.E. (2001) Characterization and functional implications of the RNA binding properties of nuclear factor TDP-43, a novel splicing regulator of CFTR exon 9. *J. Biol. Chem.*, **276**, 36337–36343.
22. Johnson, B.S., McCaffery, J.M., Lindquist, S. and Gitler, A.D. (2008) A yeast TDP-43 proteinopathy model: Exploring the molecular determinants of TDP-43 aggregation and cellular toxicity. *Proc. Natl Acad. Sci. USA*, **105**, 6439–6444.
23. Igaz, L.M., Kwong, L.K., Xu, Y., Truax, A.C., Uryu, K., Neumann, M., Clark, C.M., Elman, L.B., Miller, B.L., Grossman, M. *et al.* (2008) Enrichment of C-terminal fragments in TAR DNA-binding protein-43 cytoplasmic inclusions in brain but not in spinal cord of frontotemporal lobar degeneration and amyotrophic lateral sclerosis. *Am. J. Pathol.*, **173**, 182–194.
24. Buratti, E., Brindisi, A., Giombi, M., Tisminetzky, S., Ayala, Y.M. and Baralle, F.E. (2005) TDP-43 binds heterogeneous nuclear ribonucleoprotein A/B through its C-terminal tail: an important region for the inhibition of cystic fibrosis transmembrane conductance regulator exon 9 splicing. *J. Biol. Chem.*, **280**, 37572–37584.
25. Ayala, Y.M., Pantano, S., D'Ambrogio, A., Buratti, E., Brindisi, A., Marchetti, C., Romano, M. and Baralle, F.E. (2005) Human, Drosophila, and C.elegans TDP43: nucleic acid binding properties and splicing regulatory function. *J. Mol. Biol.*, **348**, 575–588.
26. Wang, H.Y., Wang, I.F., Bose, J. and Shen, C.K. (2004) Structural diversity and functional implications of the eukaryotic TDP gene family. *Genomics*, **83**, 130–139.
27. Igaz, L.M., Kwong, L.K., Chen-Plotkin, A., Winton, M.J., Unger, T.L., Xu, Y., Neumann, M., Trojanowski, J.Q. and Lee, V.M. (2009) Expression Of TDP-43 C-terminal fragments in vitro recapitulates pathological features of TDP-43 proteinopathies. *J. Biol. Chem.*, **284**, 8516–8524.
28. Zhang, Y.J., Xu, Y.F., Dickey, C.A., Buratti, E., Baralle, F., Bailey, R., Pickering-Brown, S., Dickson, D. and Petrucelli, L. (2007) Progranulin mediates caspase-dependent cleavage of TAR DNA binding protein-43. *J. Neurosci.*, **27**, 10530–10534.
29. Zhang, Y.J., Xu, Y.F., Cook, C., Gendron, T.F., Roettges, P., Link, C.D., Lin, W.L., Tong, J., Castanedes-Casey, M., Ash, P. *et al.* (2009) Aberrant cleavage of TDP-43 enhances aggregation and cellular toxicity. *Proc. Natl Acad. Sci. USA*, **106**, 7607–7612.
30. Nagai, Y., Tucker, T., Ren, H., Kenan, D.J., Henderson, B.S., Keene, J.D., Strittmatter, W.J. and Burke, J.R. (2000) Inhibition of polyglutamine protein aggregation and cell death by novel peptides identified by phage display screening. *J. Biol. Chem.*, **275**, 10437–10442.

INTERNAL MEDICINE

CASE REPORT

TDP-43 M337V Mutation in Familial Amyotrophic Lateral Sclerosis in Japan

Akira Tamaoka[1], Makoto Arai[2], Masanari Itokawa[2], Tetsuaki Arai[2], Masato Hasegawa[2], Kuniaki Tsuchiya[3], Hiroshi Takuma[1], Hiroshi Tsuji[1], Akiko Ishii[1], Masahiko Watanabe[1], Yuji Takahashi[4], Jun Goto[4], Shoji Tsuji[4] and Haruhiko Akiyama[2]

Abstract

The clinical features of a Japanese family with autosomal dominant adult-onset amyotrophic lateral sclerosis (ALS) are reported. Weakness initially affected the bulbar musculature, with later involvement of the extremities. Genetic studies failed to detect any mutations of the Cu/Zn superoxide dismutase-1 (SOD1) and Dynactin1 (DCTN1) genes, but revealed a single base pair change from wild-type adenine to guanine at position 1009 in TAR-DNA-binding protein (TDP-43), resulting in a methionine-to-valine substitution at position 337. The immunohistochemical study on autopsied brain of the proband's aunt showed TDP-43-positive cytoplasmic inclusions in the anterior horn cells of the spinal cord and in the hypoglossal nucleus, as well as glial cytoplasmic inclusions in the precentral gyrus, suggesting that a neuroglial proteinopathy was related to TDP-43. In conclusion, a characteristic clinical phenotype of familial ALS with initial bulbar symptoms occurred in this family with TDP-43 M337V substitution, the pathomechanism of which should be elucidated.

Key words: Amyotrophic lateral sclerosis (ALS), TAR-DNA-binding protein 43 (TDP-43)

(Inter Med 49: 331-334, 2010)
(DOI: 10.2169/internalmedicine.49.2915)

Introduction

Amyotrophic lateral sclerosis (ALS) is a progressive and fatal neurodegenerative disorder that is characterized pathologically by the degeneration of motor neurons in the brain and spinal cord, and clinically by progressive weakness and death within a few years of onset. Recently, TAR DNA-binding protein 43 (TDP-43) was identified as the major pathological protein in the motor neuron inclusions found in sporadic ALS and superoxide dismutase 1 (SOD1)-negative familial ALS, as well as in frontotemporal lobar degeneration with ubiquitin-immunoreactive, tau-negative inclusions (FTLD-U). Although the role of TDP-43 in the pathogenesis of these neurodegenerative disorders remains to be elucidated, several mutations of TDP-43 have been identified in individuals with sporadic and familial ALS, suggesting that TDP-43 may be a causative protein for these disorders (1-6). Here we first report the detailed clinical features of affected members of a Japanese family who suffered from ALS linked to TDP-43 M337V mutation.

Case Report

The proband (III-2 in Fig. 1-1) was a Japanese woman aged 61 years. She developed dysarthria at the age of 55 years, which became progressively worse. One year later, she also noted dysphagia. Neurological examination at the age of 56 revealed minimal atrophy of the facial muscles and tongue, markedly diminished reflexes of the palatal and pharyngeal muscles, and slow movements and minimal fasciculation of the tongue. Her deep tendon reflexes, including the jaw jerk, were highly exaggerated. At the age of 57, her dysphagia worsened, and atrophy and fasciculation of the

[1]Department of Neurology, Doctoral Program in Medical Sciences for Control of Pathological Processes, Graduate School of Comprehensive Human Sciences, University of Tsukuba, Tsukuba, [2]Tokyo Institute of Psychiatry, Tokyo, [3]Tokyo Metropolitan Matsuzawa Hospital, Tokyo and [4]Department of Neurology, Graduate School of Medicine, University of Tokyo, Tokyo
Received for publication September 18, 2009; Accepted for publication October 18, 2009
Correspondence to Dr. Akira Tamaoka, atamaoka@md.tsukuba.ac.jp

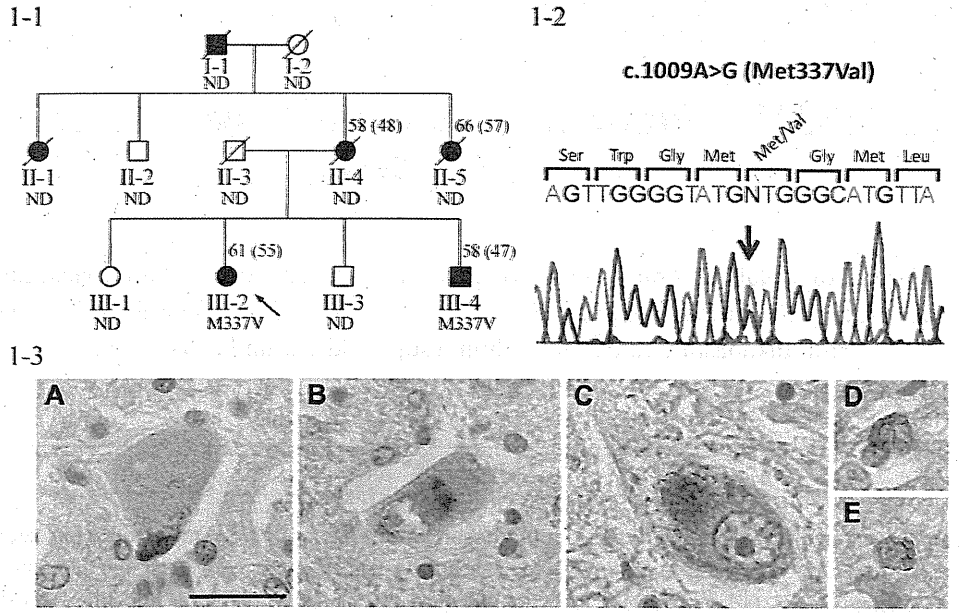

Figure 1. 1-1. Pedigree of the present family. Circles represent women and squares represent men. The slashed symbols indicate deceased subjects. Known affected persons are shown as filled symbols. The arrow represents the proband. Age at death or current age and age at disease onset in parenthesis are indicated. ND=not determined. 1-2. Chromatogram of Patient III-2 (the proband). Chromatogram shows the heterozygous sequence trace of A to G for genotyping by the reverse primer. The nucleotide position of substitution is indicated by arrow. 1-3. Immunocytochemical findings in Patient II-5. TDP-43 positive cytoplasmic inclusions in the anterior horn of the spinal cord (A, B) and in the hypoglossal nucleus (C). Glial cytoplasmic inclusions in the precentral gyrus (D, E). (A, C) Phosphorylation-independent anti-TDP-43 antibody; (B, D, E) phosphorylation-dependent anti-TDP-43 antibody (pS409/410). The sections were counterstained with hematoxylin to reveal nuclei. Bar in A=25 μm.

tongue became more prominent. Muscle weakness of the lower extremities showed slow progression, predominantly in the distal regions. At the age of 58, she was almost unable to protrude her tongue. At the age of 61, she also noted mild weakness of the upper extremities. Needle EMG showed marked neurogenic changes of the biceps, abducens pollicis brevis, vastus lateralis and tibialis anterior muscles of the right side, as well as a mild neurogenic pattern in her right masseter.

The aunt of the proband (II-5 in Fig. 1-1), a Japanese woman, developed dysarthria at the age of 57 years, followed by dysphagia, weakness of the upper extremities, and difficulty with breathing. She could walk without support until her death at the age of 66. The results of the neuropathological examination were reported in detail (7).

The younger brother of the proband (III-4 in Fig. 1-1), a Japanese man, developed dysarthiria at the age of 44 years. Neurological examination at the age of 47 showed slight dysarthria, poor movement of the soft palate, exaggerated pharyngeal reflexes and jaw jerk, slow movements, slight atrophy and fasciculation of the tongue. These findings were mainly related to pseudobulbar palsy. He also showed hyperreflexia in the upper and lower extremities (predominantly in the latter) without any pathological reflexes. Needle EMG revealed neurogenic changes of the masseter and orbicularis oris muscles, while there was a normal pattern in the tongue and extremities. He had no dysphagia, muscle weakness, or atrophy of the upper and lower extremities, as well as no sensory disturbance or vesicorectal disturbance. He could stand and walk unaided. His condition deteriorated slowly and progressively over the next 10 years. At present, he is 58 years old and virtually bed-ridden with a gastrostomy and minimal communication. Patient II-4, Patient II-1 and Patient I-1 all suffered from dysarthria until death, the details of which were unknown.

The present family demonstrated autosomal dominant inheretance of ALS and both sexes were affected. Six family members (patients I-1, II-1, II-4, II-5, III-2 and III-4) were suspected to have ALS, among whom three (II-5, III-2 and III4) had definite ALS according to the El-Escorial criteria. All six patients (2 men and 4 women) with familial ALS in this family showed dysarthria at the onset, so their clinical courses were indistinguishable from bulbar-onset ALS. There was no history of dementia and no atypical features in the kindred. Based on the information of the patients with good clinical records (patients II-4, II-5, III-2 and III-4), the mean age of symptom onset was 52.5 years (range 44-61 years) and the mean disease duration was 9.5 years (range

9-10 years) from symptom onset to death based on the outcome in patients II-4 and II-5.

After approval by the Ethics Committees of all participating institutions, sequencing of the coding regions of the TDP-43 gene in the patients (III-2 and III-4) was performed, which showed a heterozygous A-to-G transition at cDNA position 1009 (c.1009A>G) resulting in a methione-to-valine substitution at position 337 (M337V) in a highly conserved region of exon 6 (Fig. 1-2). None of the control 1,621 healthy subjects providing informed consent had this missense mutation.

Immunohistochemistry analysis of the brain of patient II-5 using both a phosphorylation-independent anti-TDP-43 antibody (10782-2-AP) and a phosphorylation-dependent anti-TDP-43 antibody (pS409/410) (8) showed neuronal cytoplasmic inclusions in the anterior horn of the spinal cord (Fig. 1-3A, B) and the hypoglossal nucleus (Fig. 1-3C), as well as glial cytoplasmic inclusions in the precentral gyrus (Fig. 1-3D, E).

Discussion

In the present study, we detected the M337V substitution in TDP-43 in a Japanese family with ALS, including one case confirmed at autopsy (patient II-5). We consider that this M337V substitution was associated with the disease, since M337V was present in two affected individuals from one generation and never in the control subjects, in addition to the fact that M337V substitution of TDP-43 has already been reported to segregate with ALS within two probably unrelated kindreds (2, 6). In a UK autosomal dominant ALS family carrying M337V substitution of TDP-43 reported by Sreedharan et al (2), three had limb-onset ALS and two had bulbar-onset ALS. The mean age of symptom onset was 47 years (range 44 to 52). Mean disease duration was 5.5 years (range 4 to 7) from symptom onset to death. The M337V mutation carrier in a US family with a strong family history of ALS reported by Rutherford et al (6) showed upper limb-onset ALS at 38 years of age, 6 years younger than the earliest onset age reported in the British M337V family (2). In the present paper, we show the first Japanese family with ALS carrying M337V substition of TDP-43, in which virtually all patients showed dysarthria at the onset, suggesting that their clinical courses were indistinguishable from bulbar-onset ALS. Among these UK, US and Japanese families carrying TDP-43 M337V mutation, the common features include no signs of dementia or other atypical features of ALS and past middle age onset of the disease. However, the signs at onset were different among these three families, and mean disease duration in the present Japanese family was longer than that in the UK family, indicating the phenotype of this mutation is quite variable. The identification of M337V in three genealogically unrelated ALS families further implies the pathogenicity of TDP-43 M337V mutation.

Regarding the pathogenecity of TDP-43 M337V mutation, Sreedharan et al (2) reported that mutant forms of TDP-43 (including M337V) fragmented *in vitro* more easily than wild-type TDP-43 and, *in vivo*, caused neuronal apoptosis and developmental delay in chick embryos, suggesting a pathophysiological link between TDP-43 and ALS. In addition, Rutherford et al (6) showed that biochemical analysis of TDP-43 in lymphoblastoid cell lines of carriers with TDP-43 mutations including M337V revealed a substantial increase in fragments possibly cleaved by caspase, including the ~25 kDa fragment, compared to control cell lines, supporting TDA-43 as a cause of ALS. Our immunohistochemical study showed TDP-43 positive cytoplasmic inclusions in the anterior horn cells of the spinal cord and in the hypoglossal nucleus, as well as glial cytoplasmic inclusions in the precentral gyrus, suggesting that a neuroglial proteinopathy was related to TDP-43. Further investigations including biochemical analysis using patients' fibroblasts or lymphoblastoid cells will be necessary to elucidate the mechanism by which TDP-43 contributes to ALS and to develop new drugs that block the pathological process related to TDP-43.

Acknowledgement

The authors thank Dr. Shuzo Shintani, Department of Neurology, Toride Kyodo Hospital and Dr. Kazuo Yoshizawa, Department of Neurology, National Hospital Organization Mito Medical Center for their clinical information on some patients of this family. This work was supported in part by grants from Ministry of Health, Labor, and Welfare, Japan and Ministry of Education, Culture, Science and Technology, Japan.

References

1. Gitcho MA, Baloh RH, Chakraverty S, et al. TDP-43 A315T mutation in familial motor neuron disease. Ann Neurol **63**: 535-538, 2008.
2. Sreedharan J, Blair IP, Tripathi VB, et al. TDP-43 mutations in familial and sporadic amyotrophic lateral sclerosis. Science **319**: 1668-1672, 2008.
3. Yokoseki A, Shiga A, Tan CF, et al. TDP-43 mutation in familial amyotrophic lateral sclerosis. Ann Neurol **63**: 538-542, 2008.
4. Kabashi E, Valdmanis PN, Dion P, et al. TARDBP mutations in individuals with sporadic and familial amyotrophic lateral sclerosis. Nat Genet **40**: 572-574, 2008.
5. Van Deerlin VM, Leverenz JB, Bekris LM, et al. TARDBP mutations in amyotrophic lateral sclerosis with TDP-43 neuropathology: a genetic and histopathological analysis. Lancet Neurol **7**: 409-416, 2008.
6. Rutherford NJ, Zhang YJ, Baker M, et al. Novel mutations in TARDBP (TDP-43) in patients with familial amyotrophic lateral sclerosis. PLoS Genetics **4**: e1000193, 2008.
7. Tsuchiya K, Shintani S, Nakabayashi H, et al. Familial amyotrophic lateral sclerosis with onset in bulbar sign, benign clinical course, and Bunina bodies: a clinical, genetic, and pathological study of a Japanese family. Acta Neuropathol **100**: 603-

607, 2000.
8. Hasegawa M, Arai T, Nonaka T, et al. Phosphorylated TDP-43 in frontotemporal lobar degeneration and amyotrophic lateral sclerosis. Ann Neurol **64**: 60-70, 2008.